NASA TN D-150

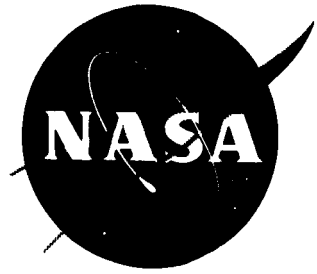

TECHNICAL NOTE

D-150

APPROXIMATE SOLUTIONS TO OPTIMUM CLIMBING TRAJECTORY

FOR A ROCKET-POWERED AIRCRAFT

By Angelo Miele and James O. Cappellari, Jr.

Purdue University

NATIONAL AERONAUTICS AND SPACE ADMINISTRATION

WASHINGTON September 1959

NATIONAL AERONAUTICS AND SPACE ADMINISTRATION

TECHNICAL NOTE D-150

APPROXIMATE SOLUTIONS TO OPTIMUM CLIMBING TRAJECTORY FOR A ROCKET-POWERED AIRCRAFT

By Angelo Miele and James O. Cappellari, Jr.

SUMMARY

The climbing program of a rocket-powered aircraft is analyzed with regard to minimum time trajectories. By using the indirect methods of the calculus of variations it is shown that, if the centripetal acceleration is neglected in the equations of motion, the totality of extremal arcs is composed of a number of constant path inclination subarcs plus one variable path inclination subarc. Under suitable hypotheses for the drag function, a solution in a closed form is obtained for the variable path inclination subarc.

For certain types of drag polars the variable path inclination subarc may split into several branches, one of which is subsonic, one transonic, and one supersonic. With regard to minimum time trajectories only the subsonic and the supersonic branch are of interest; the transition path from the former to the latter branch is studied and its optimum configuration analytically predicted.

The boundary-value problem is considered. Methods are developed for connecting the subarcs resulting from the Euler equations into the extremal arc minimizing the climbing time. The effect of important design parameters, such as wing loading or thrust loading, on the solutions is investigated.

INTRODUCTION

Several new problems of applied mathematics have arisen in the analysis of trajectories of high-speed aircraft which cannot be handled by the use of conventional methods of performance analysis. One of these problems is the determination of the optimum climbing technique from one combination of altitude and velocity to another.

In the years preceding the second World War, the optimum climbing program of piston-engine airplanes was investigated by assuming that the motion of the center of gravity of the aircraft is locally straight and

uniform. With the above hypothesis substantial simplifications were made possible, leading to simple analytical relationships of great usefulness for design purposes.

For the case of a jet-propelled aircraft, on the other hand, it becomes important to account for the inertia terms because of the high velocity of flight and its rapid variation with the altitude. Thus, the analysis of the optimum climbing technique shifts from the domain of the ordinary theory of maxima and minima into the realm of the calculus of variations.

The authors are indebted to Mr. Carlos R. Cavoti, Instructor at Purdue University, for his cooperation in some of the analyses associated with the present report.

SYMBOLS

a	speed of sound, ft sec^{-1}
$A(M)$	function defined by equation (48)
A_e	area of exit section of engine, ft^2
B	constant defined by equation (49)
$C(M)$	function defined by equation (50)
C_D	drag coefficient
C_L	lift coefficient
D	drag, lb
D_i	induced drag, lb
F	fundamental function defined by equation (9)
$G_1 \ldots G_5$	functions defined by equations (61) to (65)
g	acceleration of gravity, ft sec^{-2}
h	flight altitude, ft
h_e	energy height, ft, $h + \frac{V^2}{2g}$

H	nondimensional constant
$J_1 \ldots J_3$	first members of equations representing constraints of variational problem
K	ratio of induced drag coefficient to square of lift coefficient
L	lift, lb
m	instantaneous mass of aircraft, lb $ft^{-1}sec^2$
M	Mach number, V/a
n	quantity defined by equation (41)
p	atmospheric pressure, lb ft^{-2}
p_e	pressure in exit section of engine, lb ft^{-2}
R	air constant, $ft^2sec^{-2}\ {}^{o}R^{-1}$
S	reference surface, ft^2
t	time, sec
T	thrust, lb
V	flight velocity, ft sec^{-1}
V_e	average velocity of gases in exit section of rocket, ft sec^{-1}
α	derivative of air temperature with respect to altitude, ${}^{o}R\ ft^{-1}$
β	engine mass flow, lb $ft^{-1}sec$
γ	ratio of specific heat at constant pressure to specific heat at constant volume
$\delta(\ldots)$	variation consistent with prescribed end conditions
η	parameter
θ	path inclination with respect to a horizontal plane
$\lambda_1 \ldots \lambda_3$	Lagrange multipliers
ρ	absolute density of air, lb $ft^{-4}sec^2$
τ	absolute temperature of air, ${}^{o}R$
φ	nondimensional mass, $\frac{Hmg}{p_o S}$

Φ function defined by equation (B3), lb^{-1}

ψ function defined by equation (B4), $lb^{-1}sec^{-1}$

ω function defined by equation (B6), $lb^{-1}ft\ sec^{-1}$

Ω function defined by equation (B20), $lb^{-1}sec^{-1}$

Superscript:

$(\cdot)$ derivative with respect to time

Subscripts:

i initial condition

inc incompressible flow condition

f final condition

o sea-level condition or zero-lift condition

T transition

* condition at tropopause

– condition immediately before corner point

\+ condition immediately after corner point

OBJECT OF PRESENT RESEARCH

Preliminary variational studies by several authors, among others, Cicala and Miele (refs. 1 to 3) and Behrbohm (ref. 4), have shown that for an aircraft flying in a vertical plane the optimum paths are controlled by nonlinear systems of differential equations which are integrable, in general, only by approximate methods. Nevertheless, by making suitable assumptions, solutions in a closed form can be obtained in special cases. Up to the moment when a better understanding of the general problem is reached, these approximate solutions must be considered as an indispensable tool in the hand of the aeronautical engineer, in view of their practical importance as far as the preliminary design is concerned.

In this connection, it is to be noted that the need for an entirely new, though simplified, approach to the study of the optimum climbing technique of an aircraft was first emphasized in a paper by Lippisch (ref. 5) which was carried out as a consequence of the pioneering development of jet-propelled aircraft in Germany during World War II. Even though the above research left the bulk of variational questions associated with the climbing flight substantially unsolved, Lippisch's paper threw considerable light on a new class of problems of the mechanics of flight.

In the years following the second World War the problem of the optimum climbing program attracted considerable interest and was initially solved by assuming that the mass of the aircraft is ideally a constant (this is approximately the case with a turbojet aircraft) and the centripetal component of the acceleration is disregarded, accounting only for the tangential component. Thus, approximate solutions were detected by Miele (refs. 6 to 9) who made use of Green's theorem and by Lush (ref. 10) whose graphical-analytical method was based on the concept of energy height. In recent times, the results which Miele indicated in reference 6 were rederived by Cartaino and Dreyfus (ref. 11) along the lines of the promising theory of dynamic programming, as developed by Bellman (ref. 12).

For the case where the timewise variation of mass is important, that is, for a rocket-powered aircraft, the simplified investigation of reference 13 is to be mentioned. The present study is an extension of the theory of reference 13 and is a preliminary part to a general research program carried out under the sponsorship and with the financial assistance of the National Advisory Committee for Aeronautics. A rocket-powered aircraft operating at constant engine mass flow is considered and the induced drag is accounted for in the general treatment. Analytical methods are developed for predicting the optimum path of flight, valid for the case where both the zero-lift drag coefficient and the ratio of induced drag coefficient to square of lift coefficient are arbitrarily specified functions of the Mach number.

For certain types of drag polar the existence of two regions of best climb, one subsonic and the other one supersonic, is possible. As a consequence, a logical question is to determine the altitude at which the transition from subsonic climb to supersonic climb must be operated. Several analytical techniques are presented to handle the above question. Furthermore, methods are developed for combining the subarcs resulting from the Euler equations into the optimum configuration for minimum time of flight.

FUNDAMENTAL HYPOTHESES AND EQUATIONS OF MOTION

Hypotheses

The following hypotheses are used throughout the paper:

(1) The rocket-powered aircraft is ideally regarded as a particle of mass m variable with time t.

(2) The small angle between the thrust vector $\bar{T}$ and the velocity vector $\bar{V}$ is neglected.

(3) The aerodynamic lag is disregarded, that is, lift L and drag D forces are calculated as in unaccelerated flight.

(4) The centripetal component of the acceleration is not considered.

(5) The motion of the propellant in the piping system, in the combustion chamber, and in the nozzle is steady with respect to a reference frame rigidly connected with the solid part of the aircraft.

(6) Only flight paths contained in a vertical plane are investigated.

In view of hypotheses (1) and (2) the equation of motion on the tangent to the flight path is written as follows:

$$J_1 \equiv \dot{V} + g \sin \theta + \frac{D - T}{m} = 0 \tag{1}$$

In addition, the kinematical relationship in the vertical direction[1] is given by:

$$J_2 \equiv \dot{h} - V \sin \theta = 0 \tag{2}$$

where h denotes altitude above sea level.

With regard to the drag function, the hypothesis (3) leads to a general expression of the form:

---

[1]The kinematical relationship in the horizontal direction is not written here, since the horizontal distance does not appear anywhere in the variational problem formulated in the following sections. However, this relationship may be used a posteriori to calculate the horizontal distance flown, once the optimum path configuration has been determined.

$$D = D_o(h,V) + D_i(h,V,L) = D(h,V,L) \tag{3}$$

even accounting for compressibility and viscosity effects on the polar; on the other hand, effects of a thermal nature are not considered in the present idealized scheme.

The thrust of the rocket engine is written as:

$$T = \beta V_e + A_e(p_e - p) = T(h) \tag{4}$$

where p is outside atmospheric pressure.

Since β, V_e, and p_e are constant (hypothesis (5)) and since $p = p(h)$, one concludes that the modulus of the thrust vector is only altitude dependent. In turn, the mass m is a linear function of the time:

$$m = m_i - \beta t = m(t) \tag{5}$$

the subscript i denotes initial condition of flight $t_i = 0$.

Approximate Estimation of the Induced Drag

Some comment is here supplied about the form of the equation of motion on the normal to the flight path, used in the present report. As is known, the exact configuration of the above equation is:

$$L - m(g \cos \theta + V\dot{\theta}) = 0 \tag{6}$$

Attention should now be focused on the interaction between equations (1) and (6). The latter determines the lift required for given values of t, V, θ, and $\dot{\theta}$. In turn, lift, velocity, and altitude determine the induced drag D_i thereby enabling one to calculate the total drag of the aircraft. Once the lift is eliminated from equations (3) and (6), the drag D can be analytically represented as:

$$D = D(t,h,V,\theta,\dot{\theta}) \tag{7}$$

Now all the difficulties in treating present variational problems are essentially associated with the complicated configuration of the drag function. Solutions which are of immediate usefulness from an engineering point of view can only by achieved by renouncing equation (7) and by replacing it with a simpler analytical form, more specifically $D = D(t,h,V)$. This circumstance, in turn, implies that, to the effect

of predicting the optimum distribution of speeds versus time, equation (6) is to be abandoned and the following simplified form used in its place:

$$J_3 = L - Hmg = 0 \tag{8}$$

where H is a constant. Clearly, two approximations are embodied in equation (8), hypothesis (4) and the fact that the variable term $\cos\theta$ is replaced with a kind of average value H, where $0 \leqq H \leqq 1$.

From a conceptual point of view, the use of equation (8) in place of equation (6) is justified in all cases where the induced drag is small with respect to the zero-lift drag. For a rocket-powered aircraft this hypothesis is sound along a reasonable portion of the optimum path as the subsequent analysis shows.

Among all the values which one may attribute to the constant H, two have a special importance, $H = 1$ and $H = 0$. As a matter of fact, by setting $H = 1$ one overestimates the lift, thereby overestimating the induced drag. On the other hand, by setting $H = 0$, the opposite situation arises since the drag reduces to the zero-lift drag. Assuming that the centripetal acceleration is negligible, the optimum trajectory is, in all probability, somewhat intermediate between the two limiting ones calculated for $H = 1$ and $H = 0$.

VARIATIONAL FORMULATION

The set of equations (1), (2), and (8) is now considered where $D = D(h,V,L)$, $T = T(h)$, and $m = m(t)$. The time t is assumed as the independent variable of the problem. The dependent variables are velocity V, altitude h, path inclination θ, and lift L. Since the number of unknown functions is four, while the number of nonholonomic and holonomic constraints is three, one degree of freedom is left and an optimum requirement can be, therefore, imposed.

After prescribing the initial coordinates $t_i = 0$, $V_i = V(0)$ and $h_i = h(0)$ and the final coordinates V_f and h_f, the variational problem is formulated within the general frame of the problems of Mayer type discussed in reference 14 as follows: Among all sets of functions $V(t)$, $h(t)$, $\theta(t)$, and $L(t)$ satisfying equations (1), (2), and (8) and the prescribed end conditions, to determine that special set which minimizes the time t_f at final point.

It is to be noted that, in view of the assumed constancy for the mass flow β, the brachistocronic path is identical with the trajectory

minimizing the propellant expenditure. Furthermore, it must be pointed out that, since $\dot{\theta}$ and $\dot{L}$ do not appear anywhere in the side conditions of the problem, no requirement can be imposed on the initial and final values of θ and L. The end values for θ and L will be seen to be a mathematical consequence of the set of Euler equations.

Euler Equations

A set of variable Lagrange multipliers $\lambda_1(t)$, $\lambda_2(t)$, $\lambda_3(t)$ is introduced and the following expression, denominated fundamental function, formed:

$$F = \sum_{k=1}^{3} \lambda_k J_k \tag{9}$$

where J_1 to J_3 denote, respectively, the first members of equations (1), (2), and (8). Since the unknown functions are four in number, the extremal properties of the desired optimum trajectory are described in terms of four Euler equations, written as follows:

$$\frac{d}{dt}\left(\frac{\partial F}{\partial \dot{Z}_J}\right) - \frac{\partial F}{\partial Z_J} = 0 \qquad (J = 1,2,3,4) \tag{10}$$

where $Z_1 = V$, $Z_2 = h$, $Z_3 = \theta$, and $Z_4 = L$.

After simple manipulations the following explicit form is obtained for the Euler equations:

$$\dot{\lambda}_1 = \frac{\lambda_1}{m}\frac{\partial D}{\partial V} - \lambda_2 \sin\theta \tag{11}$$

$$\dot{\lambda}_2 = \frac{\lambda_1}{m}\left(\frac{\partial D}{\partial h} - \frac{dT}{dh}\right) \tag{12}$$

$$0 = \cos\theta\left(\lambda_1 g - \lambda_2 V\right) \tag{13}$$

$$0 = \frac{\lambda_1}{m}\frac{\partial D}{\partial L} + \lambda_3 \tag{14}$$

Discontinuity of the Eulerian Solution

The Euler equation (13) is of special interest, in that it indicates that the extremal arc is discontinuous, being generally composed of:

subarcs of equation:

$$\cos\theta = 0 \tag{15}$$

subarcs of equation:

$$\lambda_1 g - \lambda_2 V = 0 \tag{16}$$

As θ stands for flight-path inclination, equation (15) represents either a vertical dive or a vertical zoom, that is, $\theta = \mp \frac{\pi}{2}$. Equation (16), on the other hand, corresponds to a condition of motion with a continuously varying flight-path angle, as shown in the following sections of this report.

Corner Conditions

Because of the discontinuous nature of the solution the Erdmann-Weierstrass corner conditions must be applied. These are continuity conditions which must be verified at every corner of the discontinuous extremal arc by the following five quantities:

$$\frac{\partial F}{\partial \dot{V}};\ \frac{\partial F}{\partial \dot{h}};\ \frac{\partial F}{\partial \dot{\theta}};\ \frac{\partial F}{\partial \dot{L}};\ -F + \sum_{J=1}^{4}\frac{\partial F}{\partial \dot{Z}_J}\dot{Z}_J \tag{17}$$

Since the fundamental function F is independent of both $\dot{\theta}$ and $\dot{L}$, the continuity of $\frac{\partial F}{\partial \dot{\theta}}$ and $\frac{\partial F}{\partial \dot{L}}$ is automatically satisfied at all corner points. The analogous requirement associated with the remaining three quantities of equation (17) leads to:

$$(\lambda_1)_- = (\lambda_1)_+ \tag{18}$$

$$\left(\lambda_2\right)_- = \left(\lambda_2\right)_+ \tag{19}$$

$$\left[\lambda_1\left(\frac{T - D}{m} - g \sin\theta\right) + \lambda_2 V \sin\theta\right]_- = \left[\lambda_1\left(\frac{T - D}{m} - g \sin\theta\right) + \lambda_2 V \sin\theta\right]_+ \tag{20}$$

where the subscript (-) denotes a condition immediately before a corner point and the subscript (+) a condition immediately after a corner point. Thus, the Lagrange multipliers λ_1 and λ_2 must be continuous at junction points. Since thrust, drag, and mass are continuous at all time instants, the discontinuity in the path inclination θ implies that, at corner points, the following relationship must hold:

$$\left(\lambda_1 g - \lambda_2 V\right)_- = \left(\lambda_1 g - \lambda_2 V\right)_+ = 0 \tag{21}$$

Thus a corner point may lie on the subarc of equation (16) flown with variable path inclination.

Boundary Conditions

For the problem under consideration, the boundary conditions include a number of fixed end point conditions plus a number of natural conditions. The latter must be obtained from the general transversality condition, which is to be identically satisfied for all systems of variations $(\delta t, \delta z_J)$ consistent with the prescribed end conditions:

$$\left[\delta t + \left(F - \sum_{J=1}^{4} \frac{\partial F}{\partial \dot{Z}_J} \dot{Z}_J\right)\delta t + \sum_{J=1}^{4} \frac{\partial F}{\partial \dot{Z}_J} \delta Z_J\right]_i^f = 0 \tag{22}$$

The development of equation (22) leads to:

$$\left\{\left[1 - \lambda_1\left(\frac{T - D}{m} - g \sin\theta\right) - \lambda_2 V \sin\theta\right]\delta t + \lambda_1 \delta V + \lambda_2 \delta h\right\}_i^f = 0 \tag{23}$$

Since $\delta t_i = \delta V_i = \delta V_f = \delta h_i = \delta h_f = 0$ and $\delta t_f \neq 0$, one deduces that the only natural condition to be satisfied at final point is:

$$\left[1 - \lambda_1\left(\frac{T - D}{m} - g \sin\theta\right) - \lambda_2 V \sin\theta\right]_f = 0 \tag{24}$$

Notice, however, that equation (24) does not bear any further influence on the problem, essentially because the trajectory minimizing the time t_f is identical with the trajectory minimizing any multiple of the above time. The only office of the natural condition (eq. (24)), therefore, is to introduce a sort of scale factor for the distribution of Lagrange multipliers along the extremal path.

Final velocity is free of choice.- Assume now that the final altitude h_f is specified and that the final velocity V_f is not prescribed, as was previously supposed, but free of choice $\delta V_f \neq 0$. In such a case, the following natural condition:

$$\lambda_{1f} = 0 \tag{25}$$

must be satisfied in addition to equation (24). The latter can also be rewritten as

$$\lambda_{2f} = \frac{1}{(V \sin\theta)_f} \tag{26}$$

Energy height prescribed at final point.- If only the energy height $h_e = h + \frac{V^2}{2g}$ is prescribed at the final point while the individual values for h and V are not specified, the variations δh_f, δV_f must satisfy the relation:

$$\left(\delta h + \frac{V}{g}\delta V\right)_f = 0 \tag{27}$$

As a consequence, the transversality condition (23) yields the following natural condition:

$$\left(\lambda_1 g - \lambda_2 V\right)_f = 0 \tag{28}$$

which is to be satisfied in addition to equation (24).

Equations (24) and (28) can be solved in terms of the multipliers λ_1 and λ_2 as follows:

$$\lambda_{1f} = \left(\frac{m}{T - D}\right)_f \tag{29}$$

$$\lambda_{2f} = \left[\frac{mg}{V(T - D)}\right]_f \tag{30}$$

W 1 1 5

As indicated by equation (28), the final point of the extremal trajectory may lie (and, in effect, does lie) on the subarc of equation (16) flown with variable path inclination.

SUBARC FLOWN WITH VARIABLE PATH INCLINATION

Optimizing Condition

The subarc of the extremal solution defined by equation (16) is now considered and the process of elimination of the Lagrange multipliers is carried out. In this connection, the time derivative of equation (16) is calculated, yielding:

$$\dot{\lambda}_1 g - \dot{\lambda}_2 V - \lambda_2\left(\frac{T - D}{m} - g \sin\theta\right) = 0 \tag{31}$$

The four equations (11), (12), (16), and (31) can be regarded as members of an algebraic system which is linear and homogeneous in λ_1, λ_2, $\dot{\lambda}_1$, and $\dot{\lambda}_2$. As a consequence, an obvious condition for the existence of nontrivial solutions for the multipliers and their derivatives is that:

$$\begin{vmatrix} -\frac{1}{m}\frac{\partial D}{\partial V} & \sin\theta & 1 & 0 \\ \frac{1}{m}\left(\frac{dT}{dh} - \frac{\partial D}{\partial h}\right) & 0 & 0 & 1 \\ g & -V & 0 & 0 \\ 0 & g\sin\theta + \frac{D - T}{m} & g & -V \end{vmatrix} = 0 \tag{32}$$

The development of the determinant (32) leads to the following result:

$$T - D - V\frac{\partial D}{\partial V} + \frac{V^2}{g}\left(\frac{\partial D}{\partial h} - \frac{dT}{dh}\right) = 0 \tag{33}$$

which can also be rewritten as:

$$\frac{\partial\left[(T - D)V\right]}{\partial V} - \frac{V}{g}\frac{\partial\left[(T - D)V\right]}{\partial h} = 0 \tag{34}$$

Since the variational problem has one degree of freedom, one extra relation is needed, in addition to equations (1), (2), and (8), to completely characterize the solution. This extra relation is supplied by equation (15) for the constant path inclination subarcs and by equation (33) for the variable path inclination subarc. Thus, the optimizing condition is determined.

Parabolic Polar with Coefficients Depending on Mach Number

As a particular case a parabolic drag polar is now considered, that is, a polar of the form:

$$C_D = C_{Do}(M) + K(M)C_L^2 \tag{35}$$

where C_D is the total drag coefficient. Both C_{Do} and K are assumed to depend on the Mach number only. After accounting for the definitions of drag and lift, the total drag is explicitly written as:

$$D = \frac{\gamma}{2} pSC_{Do}M^2 + \frac{2}{\gamma}\frac{K}{M^2}\frac{L^2}{pS} \tag{36}$$

Atmospheric properties.- The atmosphere in which the rocket-powered aircraft is flying is represented with the following set of differential equations:

$$\frac{d\tau}{dh} = \alpha \tag{37}$$

$$\frac{dp}{dh} = -\frac{\gamma pg}{a^2} \tag{38}$$

$$\frac{d\rho}{dh} = - \frac{\gamma \rho g}{a^2} n \tag{39}$$

$$\frac{da}{dh} = \frac{\gamma R \alpha}{2a} \tag{40}$$

where

$$n = 1 + \frac{\alpha R}{g} \tag{41}$$

In the above equations p is the static pressure and $R = \frac{p}{\rho T}$, the air constant. The α variable is supposed to be a known function of the altitude.

Mach number derivatives.- Since the Mach number $M = V/a$ can be conceived as a function of velocity and altitude only, the two partial derivatives of M with respect to V and h can be calculated, yielding:

$$\frac{\partial M}{\partial V} = \frac{1}{a} \tag{42}$$

$$\frac{\partial M}{\partial h} = - \frac{M}{2} \frac{\gamma R \alpha}{a^2} \tag{43}$$

Drag and thrust derivatives.- After accounting for equations (37) to (43), the drag and thrust derivatives appearing in equation (33) can be determined. The following results are obtained:

$$\frac{V}{pS} \frac{\partial D}{\partial V} = \frac{\gamma}{2} C_{Do} M^2 \left(2 + \frac{M}{C_{Do}} \frac{dC_{Do}}{dM} \right) + \frac{2}{\gamma} \frac{K}{M^2} \left(\frac{L}{pS} \right)^2 \left(-2 + \frac{M}{K} \frac{dK}{dM} \right) \tag{44}$$

$$\frac{V^2}{g} \frac{1}{pS} \frac{\partial D}{\partial h} = - \frac{\gamma^2}{2} C_{Do} M^4 \left(n + \frac{n - 1}{2} \frac{M}{C_{Do}} \frac{dC_{Do}}{dM} \right) + 2K \left(\frac{L}{pS} \right)^2 \left(n - \frac{n - 1}{2} \frac{M}{K} \frac{dK}{dM} \right) \tag{45}$$

$$\frac{V^2}{g} \frac{1}{pS} \frac{dT}{dh} = \gamma M^2 \frac{A_e}{S} \tag{46}$$

Explicit solutions for optimum path.- In consideration of equations (44) to (46), equation (33), which describes the optimum path, can be rewritten as:

$$A(M)\left(\frac{p}{p_o}\right)^2 - B\left(\frac{p}{p_o}\right) - C(M)\left[\frac{Hmg}{p_o S}\right]^2 = 0 \tag{47}$$

where p_o is the sea-level pressure and:

$$A(M) = \frac{A_e}{S}\left(1 + \gamma M^2\right) + \frac{\gamma}{2} C_{Do} M^2 \left[3 + \gamma n M^2 + \frac{M}{C_{Do}} \frac{dC_{Do}}{dM}\left(1 + \gamma \frac{n - 1}{2} M^2\right)\right] \tag{48}$$

$$B = \frac{\beta V_e + A_e p_e}{p_o S} \tag{49}$$

$$C(M) = \frac{2}{\gamma} \frac{K}{M^2}\left[1 + \gamma n M^2 - \frac{M}{K} \frac{dK}{dM}\left(1 + \gamma \frac{n - 1}{2} M^2\right)\right] \tag{50}$$

equation (47) can be solved in terms of the ratio of static pressure at altitude to reference pressure $\frac{p}{p_o}$

$$\frac{p}{p_o} = \frac{B}{2A}\left\{1 + \sqrt{1 + 4AC\left(\frac{Hmg}{\beta V_e + A_e p_e}\right)^2}\right\} \tag{51}$$

As indicated in the section entitled "Hypotheses" the nondimensional constant appearing in the equation of motion on the normal to the flight path is $H = 0$ in the case where the variational problem is studied without accounting for the induced drag; the associated pressure-Mach number relationship is supplied by:

$$\frac{p}{p_o} = \frac{B}{A} \tag{52}$$

Once the static pressure p is known, the corresponding altitude h can be determined from the equations of the standard atmosphere. For tropospheric flight the following relationship holds:

$$h = \frac{\tau_o}{\alpha}\left[\left\{\frac{B}{2A}\left(1 + \sqrt{1 + 4AC\left[\frac{Hmg}{\beta V_e + A_e p_e}\right]^2}\right)\right\}^{1-n} - 1\right] \tag{53}$$

where τ_o is the static temperature at sea level and α the temperature-altitude derivative in the troposphere; the two functions $A(M)$ and $C(M)$ must be calculated by giving to the constant n the value which corresponds to the troposphere. When the induced drag is neglected ($H = 0$), equation (53) reduces to:

$$h = \frac{\tau_o}{\alpha}\left[\left(\frac{B}{A}\right)^{1-n} - 1\right] \tag{54}$$

With regard to stratospheric flight the static altitude is supplied by:

$$h = h_* - \frac{R\tau}{g}\,\mathrm{Log}\left[\frac{p_o}{p_*}\,\frac{B}{2A}\left(1 + \sqrt{1 + 4AC\left[\frac{Hmg}{\beta V_e + A_e p_e}\right]^2}\right)\right] \tag{55}$$

where an asterisk denotes magnitudes evaluated at the tropopause; the two functions $A(M)$ and $C(M)$ must be computed for $\alpha = 0$ and $n = 1$, in view of the fact that the static temperature τ is everywhere a constant in the stratosphere. When the induced drag is neglected ($H = 0$), the above expression reduces to:

$$h = h_* - \frac{R\tau}{g}\,\mathrm{Log}\left(\frac{p_o}{p_*}\,\frac{B}{A}\right) \tag{56}$$

Comments on solutions.- With a transformation of coordinates from the (h,V,L) space into the $\left(h_e,V,L\right)$ space, where $h_e = h + \frac{V^2}{2g}$ is the so-called energy height, equation (34) can be rewritten as:

$$\left\{\frac{\partial\left[(T - D)V\right]}{\partial V}\right\}_{\substack{h_e=\text{Constant}\\ L=\text{Constant}}} = 0 \qquad (57)$$

The above expression is the basis for an extension, to the case of a variable mass aircraft, of the energy-height method developed in reference 10 for an airplane whose mass is ideally constant; the speed for best climb is to be determined as the velocity maximizing the power excess (available power minus required power) for constant value of the energy height h_e and of the lift L (i.e., of the mass m).

With the graphical-analytical procedure associated with the energy-height method, ten or fifteen nonoptimum points must be computed for each couple of values of h_e and L as a preliminary step toward finding the optimum operating condition. With the solutions presented in the preceding section the optimum operating point is supplied by a straightforward computational technique. The advantages of the above procedure should be especially evident to the aeronautical engineer in the case where systematic design analyses are in order, such as those required to study the effect of variations in wing loading or in thrust loading on the optimum program of flight.

BOUNDARY-VALUE PROBLEM WHERE INDUCED DRAG IS NEGLECTED

With reference to the case where both the initial and final values of altitude and velocity (i.e., altitude and Mach number) are specified, the boundary-value problem is investigated. It consists of determining that combination of subarcs which satisfies a set of prescribed end conditions.

To simplify the discussion, the induced drag is neglected here ($H = 0$). Thus with regard to the altitude-Mach number plane the variable path inclination subarc is completely defined by equation (54) for tropospheric flight and equation (56) for stratospheric flight; the subarc in question shall be referred to in the following analysis as $f(M,h) = 0$, having indicated with $f(M,h)$ the function which results by calculating the difference between left and right members of either equations (54) or (56).

Notice that the curve $f(M,h) = 0$ splits the altitude-Mach number plane (fig. 1) into two regions, a region (α) bounded by h-axis and by the curve $f(M,h) = 0$; and a region (β) bounded by the M-axis and by the curve $f(M,h) = 0$. The region (α) is defined as low-speed region and (β) as high-speed region. Notice also that four different types of

boundary conditions may exist, depending upon the relative position of the initial point I and of the final point F with respect to the curve $f(M,h) = 0$. Four different solutions are accordingly found for the extremal trajectory. These solutions are indicated in table 1 and in figure 1(a), where IABF denotes the extremal arc, composed of subarcs IA, AB, and BF. The central subarc AB is always flown along the curve $f(M,h) = 0$. The initial subarc IA is a vertical dive, if point I belongs to the low-speed region (α) or a vertical zoom if point I belongs to the high-speed region (β). Analogously, the final subarc BF is a vertical zoom if point F belongs to the low-speed region (α) or a vertical dive if point F belongs to the high-speed region (β).

Problems of Conditioned Optimum

It is of interest to determine the optimum paths of flight for the case where some inequality is imposed on one or more of the variables appearing in the variational problem.

Tables 2 and 3 and figures 1(b) and 1(c) supply the solution of the minimum time problem under the limitations $h \geqq h_i$ and $h_i \leqq h \leqq h_f$, respectively. The first limitation means that the aircraft is forbidden to go to altitudes below the initial one. The second limitation means that the search of the optimum flight paths is limited to the category of arcs internal to the region of space bounded by the two horizontal planes corresponding to the initial and final altitudes. As shown in appendix A, the effect of both of the above limitations is equivalent to introducing additional subarcs of equation $h = \text{Constant}$ into the composition of the extremal path.

Effect of Induced Drag

When the so-called induced drag is accounted for ($H \neq 0$), the finding of the extremal arc associated with given end conditions becomes a little more complicated than in the case $H = 0$. This is due to the fact that equations (53) and (55) are representative of a surface in the h,M,t space, while equations (54) and (56) characterize a curve in the h,M plane.

Nevertheless, it can be said that, even in the case $H \neq 0$, all possible combinations of subarcs which may arise in solving the boundary-value problem are qualitatively the same as those covered by figure 1 for the case $H = 0$. In this connection, a typical example of computational procedure is developed in the following sections of the report.

APPLICATION OF PREVIOUS THEORY TO SPECIFIC CASES

In this section several numerical analyses are presented for typical rocket-powered aircraft configurations. The effect of variations in the basic variables of the problem are studied.

Aerodynamic Characteristics

As a basis for the analyses to follow, two hypothetical aircraft are considered. They are, respectively, denominated as configuration A and configuration B.

In figure 2 the ratio $C_{Do}/C_{Do_{inc}}$ is plotted versus Mach number M; the Mach number derivative of the above ratio versus Mach number M is plotted in figure 3. As it appears from figure 3 the main difference between configurations A and B lies in the fact that the latter shows a much steeper drag rise in the transonic region.[2]

For both configurations the ratio K/K_{inc} is assumed to depend on the Mach number M according to the data of figure 4; the Mach number derivative of the above ratio is indicated in figure 5.

Computations for Configuration A

The hypothetical aircraft denominated as configuration A is considered in this section. The low-speed aerodynamic characteristics are supposed to be such that $C_{Do_{inc}} = 0.029$ and $K_{inc} = 0.2$.

Concerning the rocket engine, it is assumed that $\beta V_e/p_o S = 0.02$ and $V_e/a_o = 7$. For simplicity the ratio A_e/S is regarded as negligible, in view of the qualitative character of the present set of examples.

Variable path inclination subarc.- Attention is now focused on the subarc of the extremal solution discussed earlier.

As a first step, the two functions A(M) and C(M), (defined by eqs. (48) and (50)) are calculated and plotted in figures 6 and 7 for both tropospheric flight and stratospheric flight. As a second step,

---

[2]This circumstance affects in a substantial way the optimum technique of flight, as it is shown in the following examples.

the relationship between h, M and $\varphi = Hmg/p_oS$ is calculated and plotted for tropospheric flight (eq. (53)) and stratospheric flight (eq. (55)) in figure 8.

In the case where the variational problem is solved without accounting for the induced drag, the condition $H = 0$ must be imposed. As a consequence, the variable path inclination subarc is represented by that curve $h(M)$ of figure 8 which corresponds to $\varphi = 0$.

If, on the other hand, the induced drag is accounted for and if (for instance) the equation of motion on the normal to the flight path is written as $L - mg = 0$, then the condition $H = 1$ must be imposed. It is to be noted, however, that the mass of the aircraft is a linear function of time; as a consequence, the parameter φ is also linearly variable with time. From this consideration it follows that the actual curve $h(M)$, which is representative of the optimum technique of flight in the (h,M) plane, does not follow any of the $\varphi = \text{Constant}$ curves sketched in figure 8, but rather crosses them (in the sense of decreasing values of φ) as the flight program develops.

Figure 8(a) shows that the effect of the induced drag on the optimum altitude-Mach number distribution is, from an engineering point of view, negligible for tropospheric flight. The same effect, however, may become important for flight in the stratosphere (fig. 8(b)) depending upon the value of the instantaneous wing loading (for a given thrust loading) and upon the flight Mach number.

Extremal arc for one specific set of boundary conditions.- The following set of end conditions is now considered: $M_i = 0.4$, $h_i = 0$, $\varphi_i = 0.03$, $M_f = 1.4$, $h_f = 35{,}332$ ft. The optimum path is investigated under the limitation $h_i \leqq h \leqq h_f$.

In accordance with the data of figures 1(c) and 8(a) the extremal arc includes one initial subarc IA flown in level flight, one central subarc AB flown with variable path inclination and variable altitude, and one final subarc BF, also flown in level flight. A computation procedure is now developed, specially suitable to the present set of end conditions (flight condition of type I, $h_i \leqq h \leqq h_f$).

Initial subarc IA.- Simple transformations of the equations of motion show that the path of the aircraft can be complexly described in terms of the three variables h, M, and $\varphi = Hmg/p_oS$. For the case of level flight, the differential relationship to be integrated is:

$$\frac{dM}{d\varphi} = \frac{p_o S}{\alpha\beta}\left\{\frac{1}{\varphi}\left[\frac{p}{p_o}\left(\frac{\gamma}{2} C_{Do} M^2 + \frac{A_e}{S}\right) - B\right] + \frac{2}{\gamma}\frac{K}{M^2}\varphi\frac{p_o}{p}\right\} \tag{58}$$

where the additional constraint $p = \text{Constant}$ is to be considered. For the initial conditions of the preceding section, one must assume $p = p_i = p_o$.

Corner point A.- In consideration of the fact that corner point A belongs to both subarcs IA and AB, and that its altitude is known $(h_A = 0)$, the two remaining coordinates M_A and φ_A must be found as follows: the curve $\varphi(M)$, which results by forward integration of equation (58) started at point I, must be intersected with the curve $\varphi(M)$ which results by imposing the condition $p/p_o = 1$ into equation (47):

$$\varphi = \sqrt{\frac{A - B}{C}} \tag{59}$$

Both equations (58) and (59) are plotted in figure 9, where the corner point A is shown $(\varphi_A = 0.0291, \quad M_A = 0.557)$.

Central subarc AB.- For the subarc AB of the extremal path the equations of motion must be considered, subject to the constraint represented by equation (47).

After laborious transformations (omitted for the sake of brevity) the following differential relationship may be obtained between Mach number and altitude:

$$\frac{dM}{d\left(h\frac{g}{a_o^2}\right)} = -\frac{G_1 G_2 + G_3}{G_1 G_4 + G_5} \tag{60}$$

where

$$G_1 = B\left(1 + \frac{2}{\gamma}\frac{K}{M^2}\frac{1}{C}\right) - \frac{p}{p_o}\left(\frac{A_e}{S} + \frac{\gamma}{2} C_{Do} M^2 + \frac{2}{\gamma}\frac{K}{M^2}\frac{A}{C}\right) \tag{61}$$

$$G_2 = -\gamma\left(\frac{a_o}{a}\right)^2 \frac{A\,\frac{p}{p_o} - \frac{B}{2}}{A\,\frac{p}{p_o} - B} \tag{62}$$

$$G_3 = \frac{1}{M}\,\frac{a_o}{a}\,\frac{\beta a_o}{p_o S}\left(1 + \gamma\,\frac{n-1}{2}\,M^2\right) \tag{63}$$

$$G_4 = \frac{1}{2}\left(\frac{\frac{p}{p_o}\,\frac{dA}{dM}}{A\,\frac{p}{p_o} - B} - \frac{1}{C}\,\frac{dC}{dM}\right) \tag{64}$$

$$G_5 = \frac{a}{a_o}\,\frac{\beta a_o}{p_o S} \tag{65}$$

A forward integration of equation (60) started at point A, yields the Mach number-altitude distribution along the subarc AB (fig. 10(a)). The integration process must be discontinued at the altitude $h_B = h_f$. Once the $h(M)$ relationship is known, the distribution of mass (fig. 10(b)) is supplied by:

$$\varphi = \sqrt{\frac{p}{p_o}\,\frac{1}{C}}\,\sqrt{A\,\frac{p}{p_o} - B} \tag{66}$$

The coordinates of corner point B are the following: $M_B = 0.89$, $\varphi_B = 0.0210$, $h_B = 35{,}332$ ft.

Final subarc BF.- For the particular example under consideration, the final subarc BF is to be flown at constant altitude. The Mach number-mass distribution is obtained by integrating equation (58), subject to the constraint $p = p_f$.

Both the subarc BF and the complete trajectory IABF are represented in the altitude-Mach number plane and in the mass-Mach number plane in figure 10.

Computations for Configuration B

The hypothetical aircraft designated as configuration B is now considered. The following nondimensional parameters characterize the aircraft and the engine: $C_{Do_{inc}} = 0.029$, $K_{inc} = 0.2$, $V_e/a_o = 7$, $A_e/S \cong 0$.

Unless stated otherwise, the thrust loading is assumed such that $\beta V_e/p_o S = 0.02$ and the so-called induced drag is neglected. All comparisons between configuration A and configuration B are made on a zero-lift drag basis.

General remarks on variable path inclination subarc.- The important function $A(M)$, which is defined by equation (48), is plotted in figure 11 for both tropospheric and stratospheric flight. In turn, the altitude-Mach number distribution (eqs. (54) and (56)) is indicated in figure 12.

A comparison between figures 8 (induced drag neglected, $\varphi = 0$) and 12 emphasizes the main difference between configurations A and B. Configuration A (mild drag gradient in the transonic region) yields a single-valued relationship $M(h)$, while configuration B (steep drag gradient in the transonic region) yields a multiple-valued relationship $M(h)$ in the altitude interval between 55,000 and 78,000 feet.

More specifically, associated with configuration B (fig. 12) are three branches of the solution, a subsonic branch (solid line), a transonic branch (dotted line), and a supersonic branch (solid line). By means of Green's theorem, as in reference 6, it can be proved that the transonic branch is associated with maximum time solutions, while both the subsonic and the supersonic branch are associated with minimum time solutions.

The next question is then to establish whether climbing must be performed at subsonic or supersonic speed or by using a combined subsonic-supersonic technique of flight. In the latter case, it is relevant to determine the special altitude at which the rocket-powered aircraft is to be transferred from the subsonic to the supersonic branch of the solution.

Effect of thrust loading on variable path inclination subarc.- To investigate the effect of variations in thrust loading on the solutions, three values are considered for the parameter $\beta V_e/p_o S$, namely 0.01, 0.02, and 0.03. The associated Mach number-altitude distribution for the subsonic and supersonic branches of the solution is illustrated in figure 13.

In both instances, the effect of increasing the thrust is to increase the optimum Mach number at a given altitude. For the subsonic branch this increase in the Mach number is decidedly more pronounced at the lower altitudes, becoming rather slight at the higher altitudes. In the supersonic domain, the increase is almost uniform through the given Mach number and altitude range.

Extremal path for one specific set of boundary conditions.- The following set of end conditions is now considered: $M_i = 0.545$, $h_i = 0$, $m_i g/S = 60$ lb ft^{-2}; $M_f = 2$, $h_f = 70{,}000$ ft and the limitation $h_i \leq h \leq h_f$ is imposed.

The end conditions are such (fig. 14) that the initial point I and the corner point A are coincident in the altitude-Mach number plane $I \equiv A$. Thus, the amplitude of the initial subarc IA shrinks to zero and the optimum path reduces to a composite subarc ACDB, followed by a level flight subarc BF.

In turn, the composite subarc ACDB embodies three parts, one variable path inclination subarc AC flown along the subsonic branch of equation (52), one variable path inclination subarc DB flown along the supersonic branch of equation (52), and one transition subarc CD.

With regard to the transition subarc CD, the present analysis is circumscribed here to only those subarcs which are flown in level flight. For the latter, the best transition altitude h_T is to be such that $\Omega(h_T) = 0$, where the function Ω is defined by equation (B20) of appendix B.

Numerical computations show that $(h_T)_{opt} = 58{,}800$ ft and this fact is clearly indicated in figure 15 where the function Ω is plotted versus the transition altitude h_T.

When induced drag is accounted for, the extremal path modifies. Admitting, for simplicity, that the optimum transition altitude does not change because of induced drag effect, the analysis indicates that the new extremal arc is the trajectory IA'C'D'B'F of figure 14.

The induced drag causes only a minor shifting of the optimum distribution of speed with respect to the other distribution calculated for zero induced drag. This result is largely due to the relatively low initial wing loading considered in the preceding section. Considerably larger effects must be expected for initial wing loadings of the order of 100 lb ft^{-2}.

Comparison between optimum transition subarc and neighboring paths.- In order to study the effect of deviations of the actual transition altitude with respect to the optimum value predicted in the previous section, the following example is carried out.

The initial condition of flight is assumed to be such that $h_i = 0$, $M_i = 0.545$, $m_i g/S = 60$ lb ft^{-2}, and the initial point I is identical with the corner point A since I is located on the subsonic branch of the variable path inclination subarc (fig. 12).

Four different final conditions of flight are considered; however, all of them are chosen in such a way that the final point F is located on the supersonic branch of the variable path inclination subarc. As a consequence, the final point F and the corner point B are identical.

Paths of the form IACDBF ($I \equiv A$, $B \equiv F$) are considered (fig. 12) including one climbing maneuver AC performed along the subsonic branch of the variable path inclination subarc and one climbing maneuver DB performed along the supersonic branch of the variable path inclination subarc. Intermediate between the above two climbing subarcs is one transition path CD, which is assumed to occur at constant altitude h_T.

In figure 16 the time t_f necessary to reach the desired final condition of flight is plotted as a function of the actual transition altitude h_T. From this graph the conclusion is reached that a reasonable deviation in transition altitude with respect to the optimum value $(h_T)_{opt}$ does not cause a substantial change in the time t_f. The transition problem, therefore, is not a critical one for rocket-powered aircraft.[3]

REMARKS ON DISCONTINUOUS NATURE OF SOLUTIONS

It has been seen in the preceding analyses that there exist discontinuities in the path inclination at the corner points where the vertical dive or vertical zoom subarcs join the variable path inclination subarcs and where the horizontal transition subarcs join the variable path inclination subarcs. These discontinuities are a mathematical

---

[3]Computations, omitted for the sake of brevity, have been carried out for the case where the induced drag is accounted for. The qualitative conclusions are essentially the same as in the case where the induced drag is neglected.

consequence of hypothesis (4), which neglects the centripetal component of the acceleration. Of course, such discontinuities are not physically possible during actual flight operations. Thus, in any application of these methods, the actual flight path must be faired in the vicinity of each corner point so as to continuously join the different subarcs. Such fairings should be consistent with the structural capacity of the aircraft and with the physiological ability of the pilot to withstand acceleration. Moreover, they should be consistent with the thrust-drag characteristics of the aircraft.

CONCLUSIONS

The climbing technique for a rocket-powered aircraft is analyzed from the standpoint of minimizing the time required to fly from one combination of speed and altitude to another. It is shown that the totality of extremal arcs includes a number of constant path inclination subarcs and a number of variable path inclination subarcs.

Concerning the latter, solutions in a closed form are developed. Depending upon the type of drag polar, the Mach number-altitude relationship can either be of the single valued type or of the multiple-valued type. In this second case three branches generally exist for the solution, a subsonic branch, a transonic branch which is of no interest for flight operations, and a supersonic branch.

The optimum altitude for the transition from the subsonic to the supersonic branch of the solution is determined. With regard to the boundary-value problem, several numerical examples are presented, having the effect of illustrating the general procedures developed in the present report.

Purdue University,
Lafayette, Ind., November 8, 1957.

APPENDIX A

ON THE COMPOSITION OF EXTREMAL PATH WHEN INEQUALITY OF FORM $h_i \leqq h \leqq h_f$ IS IMPOSED ON VARIATIONAL PROBLEM

In the main text it was stated that, if the inequality $h_i \leqq h \leqq h_f$ is imposed upon the class of paths which are subject to the variational investigation, additional subarcs of the form h = Constant are introduced into the composition of the extremal arc. This statement is now supported with the following process of reasoning.

When, in a certain variational question, one of the variables is subject to some inequality which results from the characteristic conditions of the problem, the inherent information is to be translated into the setting of the question at the very beginning, otherwise the solution may not be consistent with the desired limitation. In this connection, it is of interest to exploit the artifice of parametric representation of the variable involved in the inequality. Such a technique was originally introduced in reference 15 in a problem of optimum burning program; its main effect consists in treating a constraint involving an inequality under the same analytical procedures developed for a constraint represented by an equality.

The flight altitude h is represented as a function of a parameter η (fig. 17) where

$-\infty \leqq \eta \leqq \eta_1$ the altitude is $h = h_i$

$\eta_2 \leqq \eta \leqq \infty$ the altitude is $h = h_f$

$\eta_1 \leqq \eta \leqq \eta_2$ a one-to-one correspondence is assumed between h and η.

With the above scheme η is considered as an independent parameter, as far as the flight altitude is concerned, and is allowed to vary between $-\infty$ and ∞. The variable h becomes a dependent quantity, varying between h_i and h_f according to the scheme shown in figure 17.

Notice that $\frac{dh}{d\eta} = 0$ represents either a level flight condition $h = h_i$ or a level flight condition $h = h_f$. On the other hand, $\frac{dh}{d\eta} \neq 0$ is representative of any other operating condition of the aircraft at

altitudes which are intermediate between the two limiting ones. Notice also that η is only a parameter and that there is no necessity of attributing to it any special physical meaning.

The time derivative of the flight altitude is written as:

$$\dot{h} = \frac{dh}{d\eta}\,\dot{\eta} \tag{A1}$$

and, as a consequence, the fundamental function F modifies as follows:

$$F = \lambda_1\left(\dot{V} + g \sin\theta + \frac{D - T}{m}\right) + \lambda_2\left(\frac{dh}{d\eta}\,\dot{\eta} - V \sin\theta\right) + \lambda_3\left(L - Hmg\right) \tag{A2}$$

The independent variable of the variational problem is the time t. The dependent variables are now V, η (in place of h), θ, and L. The three Euler equations associated with V, θ, and L are still supplied by equations (11), (13), and (14). On the other hand, the Euler equation associated with the new variable η is written as follows:

$$\frac{d}{dt}\left(\frac{\partial F}{\partial \dot{\eta}}\right) - \frac{\partial F}{\partial \eta} = 0 \tag{A3}$$

where:

$$\frac{\partial F}{\partial \eta} = \frac{\lambda_1}{m}\left(\frac{\partial D}{\partial h} - \frac{dT}{dh}\right)\frac{dh}{d\eta} + \lambda_2\dot{\eta}\,\frac{d^2h}{d\eta^2} \tag{A4}$$

$$\frac{\partial F}{\partial \dot{\eta}} = \lambda_2\,\frac{dh}{d\eta} \tag{A5}$$

$$\frac{d}{dt}\left(\frac{\partial F}{\partial \dot{\eta}}\right) = \dot{\lambda}_2\,\frac{dh}{d\eta} + \lambda_2\,\frac{d^2h}{d\eta^2}\,\dot{\eta} \tag{A6}$$

From equations (A3) to (A6) one obtains:

$$\frac{dh}{d\eta}\left[\dot{\lambda}_2 - \frac{\lambda_1}{m}\left(\frac{\partial D}{\partial h} - \frac{dT}{dh}\right)\right] = 0 \tag{A7}$$

Equation (A7) splits into the following two solutions:

$$\dot{\lambda}_2 - \frac{\lambda_1}{m}\left(\frac{\partial D}{\partial h} - \frac{dT}{dh}\right) = 0 \tag{A8}$$

$$\frac{dh}{d\eta} = 0 \tag{A9}$$

Equation (A8) is identical with equation (12). Equation (A9), in turn, yields the two extra subarcs $h = h_i$ and $h = h_f$, as is clear from the device of parametric representation illustrated in figure 17.

APPENDIX B

ANALYSIS OF TRANSITION SUBARC

In the main text the transition problem was posed: For certain types of drag polars the variable path inclination subarc may split into two useful portions, that is, a subsonic branch and a supersonic branch. This circumstance causes the following question to arise: What is the best transition maneuver (from a time standpoint) in order to transfer the aircraft from the subsonic branch to the supersonic branch of the solution?

In the present appendix an attempt is carried out to supply an engineering answer to the above problem. The analysis is circumscribed from start to the class of transition subarcs which are flown in level flight. Induced drag effects are neglected.

Assume that the boundary conditions are as in figure 18, the initial point I corresponding to low subsonic speed is located, in the velocity-altitude plane, on the left with respect to the subsonic branch of the solution with variable path inclination; the final point F corresponding to high supersonic speed is located on the right of the supersonic branch of the solution with variable path inclination. Assume also that the limitation $h_i \leqq h \leqq h_f$ is imposed and consider the family of trajectories IACDBF. Each element of the above family is composed of five subarcs:

(1) Subarc IA flown in level flight at $h = h_i$

(2) Subarc AC flown along the subsonic branch of the solution with variable path inclination (eq. (52))

(3) Transition subarc CD flown in level flight at $h = h_T$

(4) Subarc DB flown along the supersonic branch of the solution with variable path inclination (eq. (52))

(5) Subarc BF flown in level flight at $h = h_f$

It is clear that, for the previously defined family of trajectories, the time t_f necessary to reach the desired final point is only a function $t_f(h_T)$ of the transition altitude h_T. It follows that the optimum transition subarc is the one for which the following relation of the ordinary theory of maxima and minima is satisfied:

$$\frac{dt_f}{dh_T} = 0 \tag{B1}$$

Time Interval from Initial Point to Final Point

Simple transformations of equations (1), (2), and (5) yield the following differential relationship (the induced drag is neglected):

$$\frac{dt}{m_i - \beta t} = \psi\, dh + \Phi\, dV \tag{B2}$$

$$\Phi = \frac{1}{T - D_o} = \Phi(h,V) \tag{B3}$$

$$\psi = \frac{g}{V(T - D_o)} = \psi(h,V) \tag{B4}$$

whose corresponding integral form is:

$$t_f = \frac{m_i}{\beta}\left[1 - \exp(-\beta\omega)\right] \tag{B5}$$

$$\omega = \int_{IACDBF} (\psi\, dh + \Phi\, dV) \tag{B6}$$

The derivative of the time t_f with respect to the transition altitude h_T is supplied by:

$$\frac{dt_f}{dh_T} = m_i \exp(-\beta\omega)\, \frac{d\omega}{dh_T} \tag{B7}$$

and, as a consequence, the condition (B1) is equivalent to:

$$\frac{d\omega}{dh_T} = 0 \tag{B8}$$

Application of Theorem of Derivation Under Integral Sign

The line integral (B6) can be broken into five parts, each associated with a different subarc of the family of trajectories under consideration:

$$\omega = \omega_{IA} + \omega_{AC} + \omega_{CD} + \omega_{DB} + \omega_{BF} \tag{B9}$$

$$\omega_{IA} = \int_{IA} \Phi \, dV \tag{B10}$$

W
1
1
5

$$\omega_{AC} = \int_{AC} (\psi \, dh + \Phi \, dV) \tag{B11}$$

$$\omega_{CD} = \int_{CD} \Phi \, dV \tag{B12}$$

$$\omega_{DB} = \int_{DB} (\psi \, dh + \Phi \, dV) \tag{B13}$$

$$\omega_{BF} = \int_{BF} \Phi \, dV \tag{B14}$$

A change in the transition altitude h_T causes a change in the integrals (B11) to (B13) because the limits of integration and/or the integrand function are affected. The following results are consequently obtained:

$$\frac{d\omega_{IA}}{dh_T} = 0 \tag{B15}$$

$$\frac{d\omega_{AC}}{dh_T} = \left(\psi_C + \Phi_C \frac{dV_C}{dh} \right)_{h=h_T} \tag{B16}$$

$$\frac{d\omega_{CD}}{dh_T} = \left(\int_{V_C}^{V_D} \frac{\partial \Phi}{\partial h} \, dV + \Phi_D \frac{dV_D}{dh} - \Phi_C \frac{dV_C}{dh} \right)_{h=h_T} \tag{B17}$$

$$\frac{d\omega_{DB}}{dh_T} = -\left(\psi_D + \Phi_D \frac{dV_D}{dh} \right)_{h=h_T} \tag{B18}$$

$$\frac{d\omega_{BF}}{dh_T} = 0 \tag{B19}$$

From equations (B8) and (B15) to (B19) the following fundamental result arises:

$$\Omega(h_T) \equiv \left(\psi_C - \psi_D + \int_{V_C}^{V_D} \frac{\partial \Phi}{\partial h} \, dV \right)_{h=h_T} = 0 \tag{B20}$$

The above equation implicitly defines the optimum transition height $(h_T)_{opt}$ and it must be solved, in general, by approximate methods.

Application of Green's Theorem

The result represented by equation (B20) can also be achieved by means of a radically different technique based on the use of Green's theorem.

Consider (fig. 18) two alternate trajectories, namely the path IACDBF whose transition subarc CD is flown at altitude h_T and the path IAC'D'BF whose transition subarc C'D' is flown at altitude $h'_T = h_T + \Delta h_T$. For the former trajectory the function ω is supplied by equation (B6). With regard to the latter trajectory the function ω is given by:

$$\omega' = \int_{IAC'D'BF} (\psi \, dh + \Phi \, dV) \tag{B21}$$

The increment $\Delta\omega$ associated with the increment Δh_T of the transition altitude can now be expressed in the form of a cyclic integral:

$$\Delta\omega = \omega' - \omega = \oint_{CC'D'DC} (\psi \, dh + \Phi \, dV) \tag{B22}$$

In turn, the above line integral can be transformed by means of Green's theorem into a surface integral associated with the area α bounded by the clockwise circuit CC'D'DC:

$$\Delta\omega = - \iint_{\alpha} \left(\frac{\partial \psi}{\partial V} - \frac{\partial \Phi}{\partial h} \right) dV \, dh \tag{B23}$$

Consider, now, a set of smaller and smaller increments Δh_T. In the limit Δh_T shrinks into the infinitesimal increment dh_T; as a consequence, $\Delta\omega$ tends to $d\omega$, the latter quantity being supplied by:

$$d\omega = dh_T \left[\int_{V_C}^{V_D} \left(\frac{\partial \Phi}{\partial h} - \frac{\partial \psi}{\partial V} \right) dV \right]_{h=h_T} \tag{B24}$$

The condition (B8) is, therefore, equivalent to:

$$\left[\int_{V_C}^{V_D} \left(\frac{\partial \Phi}{\partial h} - \frac{\partial \psi}{\partial V} \right) dV \right]_{h=h_T} = 0 \tag{B25}$$

Since the above line integral is to be computed at constant altitude, the following relationship holds:

$$\left(\int_{V_C}^{V_D} \frac{\partial \psi}{\partial V} \, dV \right)_{h=h_T} = \left(\psi_D - \psi_C \right)_{h=h_T} \tag{B26}$$

The combination of equations (B25) and (B26) yields once more the fundamental equation:

$$\left(\psi_C - \psi_D + \int_{V_C}^{V_D} \frac{\partial \Phi}{\partial h} \, dV \right)_{h=h_T} = 0 \qquad \text{(B27)}$$

The same result has been obtained by the writers starting from the Erdmann-Weierstrass corner conditions. The demonstration is omitted for brevity.

REFERENCES

1. Cicala, P., and Miele, A.: Evoluzioni Brachistocrone di un Aereo. Atti della Accademia delle Scienze di Torino, vol. 89, 1954-1955.

2. Cicala, P., and Miele, A.: Brachistocronic Manoeuvers of a Constant Mass Aircraft in a Vertical Plane. Jour. Aero. Sci., vol. 22, no. 4, Apr. 1955, pp. 286-288.

3. Cicala, P., and Miele, A.: Brachistocronic Manoeuvres of a Variable Mass Aircraft in a Vertical Plane. Jour. Aero. Sci., vol. 22, no. 8, Aug. 1955, pp. 577-578.

4. Behrbohm, H.: Optimal Trajectories in the Vertical Plane, SAAB Tech. Note No. 34, 1955.

5. Lippisch, A.: Flugmechanische Beziehungen der Flugzeuge mit Strahlantrieb. Trans. Rep. No. F-TS-685-RE Headquarters AMC, Dayton, Ohio, Oct. 1946.

6. Miele, A.: Problemi di Minimo Tempo nel Volo Non-Stazionario degli Aeroplani. Atti della Accademia delle Scienze di Torino, vol. 85, 1950-1951, pp. 41-52.

7. Miele, A.: Soluzioni Generali di Problemi di Ottimo in Volo Non-Stazionario. L'Aerotecnica, vol. 32, no. 3, 1952, pp. 135-142. (Also available as NACA TM 1388.)

8. Miele, A.: Traiettorie Ottime di Volo degli Aeroplani Azionati da Turboreattori, L'Aerotecnica, vol. 32, no. 4, 1952, pp. 206-219. (Also available as NACA TM 1389.)

9. Miele, A.: On the Non-Steady Climb of Turbo-Jet Aircraft. Jour. Aero. Sci., vol. 21, no. 11, Nov. 1954, pp. 781-783.

10. Lush, K. J.: A Review of the Problem of Choosing a Climb Technique, with Proposals for a New Climb Technique for High Performance Aircraft. R. M. 2557, Brit. A.R.C., 1951.

11. Cartaino, T. F., and Dreyfus, S. E.: Application of Dynamic Programming to the Airplane Minimum Time-to-Climb Problem. Rep. P-834 (Revised), The Rand Corp., Jan. 1957.

12. Bellman, Richard.: Dynamic Programming of Continuous Processes. Rep. R-271, The Rand Corp., July 1954.

13. Miele, A.: Optimum Climbing Technique for a Rocket-Powered Aircraft. Jet Propulsion, vol. 25, no. 8, Aug. 1955, pp. 385-391.

14. Bliss, G. A.: Lectures on the Calculus of Variations. The Univ. of Chicago Press, 1946.

15. Miele, A.: An Extension of the Theory of the Optimum Burning Program for the Level Flight of a Rocket-Powered Aircraft. Tech. Note 56-302, Contract AF-18(603)-69 Office Sci. Res. and Purdue University, June 1956.

TABLE 1.- COMPOSITION OF EXTREMAL ARC WHEN NO LIMITATION IMPOSED ON FLIGHT PATH

Flight conditions	Region where point I belongs	Region where point F belongs	Subarc IA	Subarc AB	Subarc BF
I	α	β	$\theta = -\pi/2$	$f(M,h) = 0$	$\theta = -\pi/2$
II	α	α	$\theta = -\pi/2$	$f(M,h) = 0$	$\theta = \pi/2$
III	β	α	$\theta = \pi/2$	$f(M,h) = 0$	$\theta = \pi/2$
IV	β	β	$\theta = \pi/2$	$f(M,h) = 0$	$\theta = -\pi/2$

TABLE 2.- COMPOSITION OF EXTREMAL ARC UNDER LIMITATION $h \geqq h_i$

Flight conditions	Region where point I belongs	Region where point F belongs	Subarc IA	Subarc AB	Subarc BF
I	α	β	$h = h_i$	$f(M,h) = 0$	$\theta = -\pi/2$
II	α	α	$h = h_i$	$f(M,h) = 0$	$\theta = \pi/2$
III	β	α	$\theta = \pi/2$	$f(M,h) = 0$	$\theta = \pi/2$
IV	β	β	$\theta = \pi/2$	$f(M,h) = 0$	$\theta = -\pi/2$

TABLE 3.- COMPOSITION OF EXTREMAL ARC UNDER LIMITATION $h_i \leqq h \leqq h_f$

Flight condition	Region where point I belongs	Region where point F belongs	Subarc IA	Subarc AB	Subarc BF
I	α	β	$h = h_i$	$f(M,h) = 0$	$h = h_f$
II	α	α	$h = h_i$	$f(M,h) = 0$	$\theta = \pi/2$
III	β	α	$\theta = \pi/2$	$f(M,h) = 0$	$\theta = \pi/2$
IV	β	β	$\theta = \pi/2$	$f(M,h) = 0$	$h = h_f$

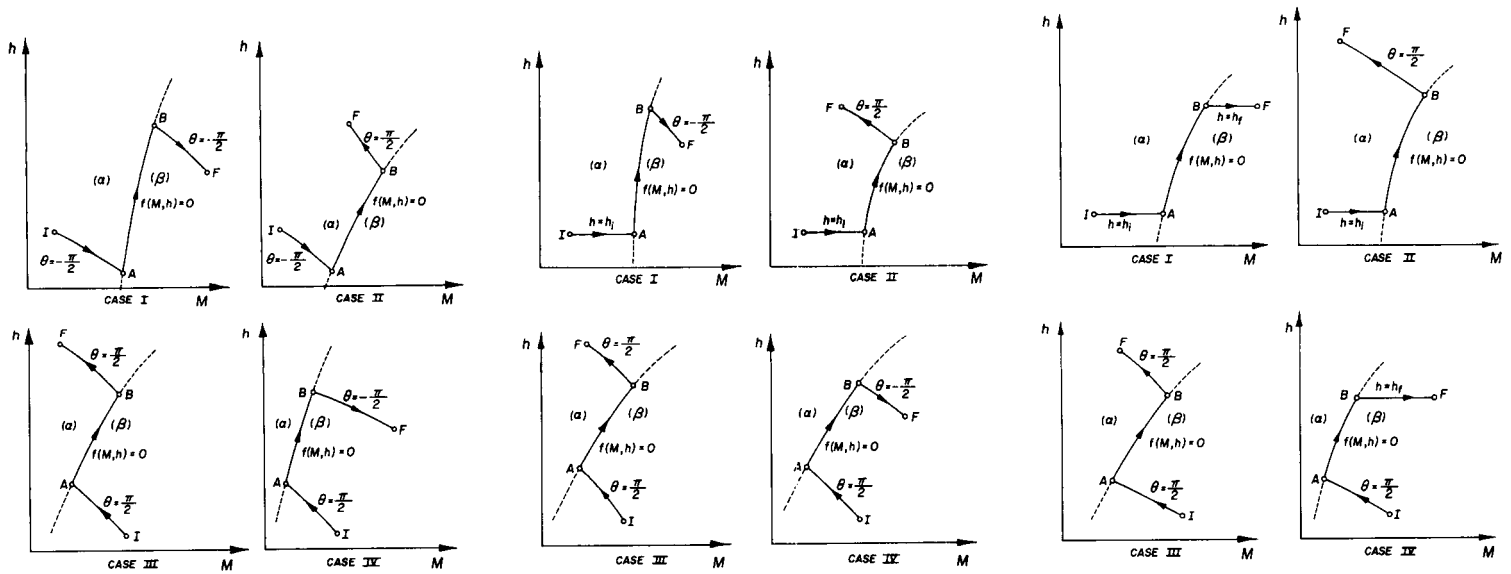

(a) General case. (b) $h \geqq h_i$. (c) $h_f \geqq h \geqq h_i$.

Figure 1.- Optimum Mach number-height relationship.

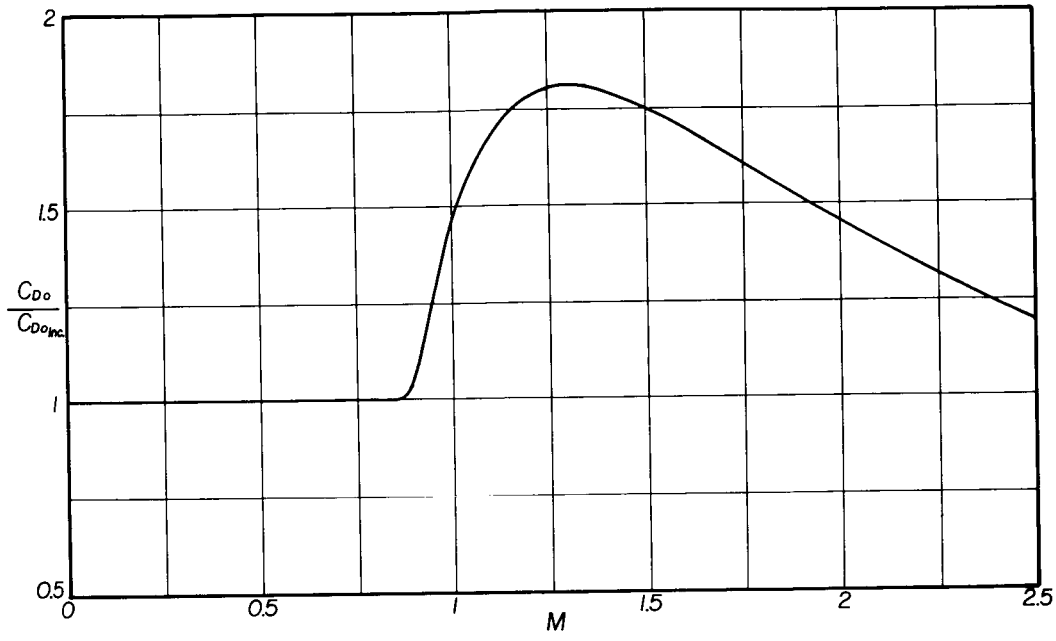

(a) Configuration A.

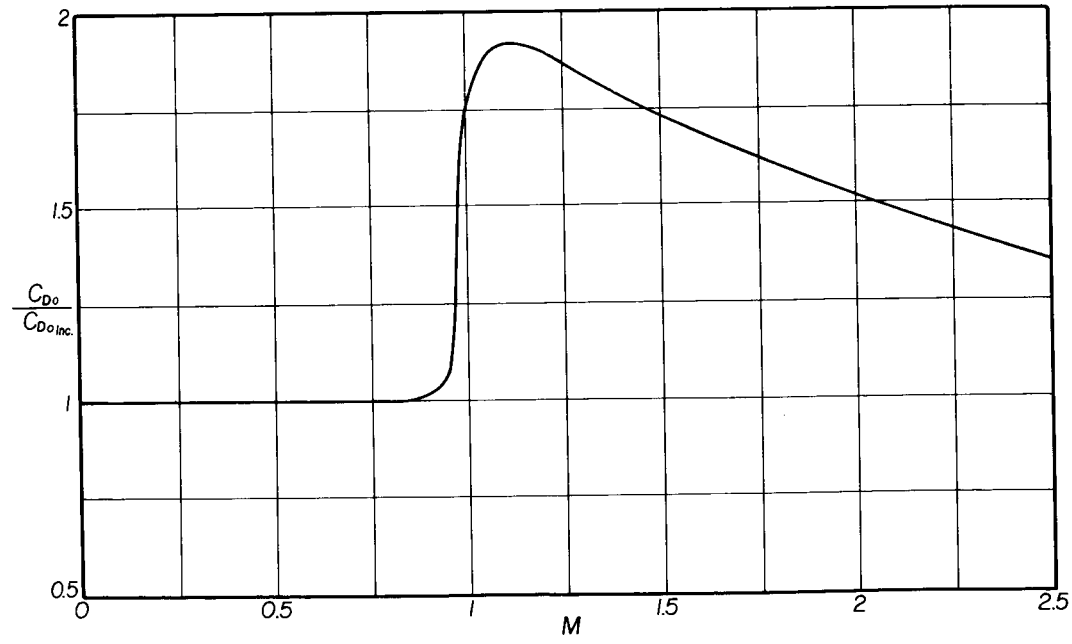

(b) Configuration B.

Figure 2.- Zero-lift drag coefficient as a function of Mach number.

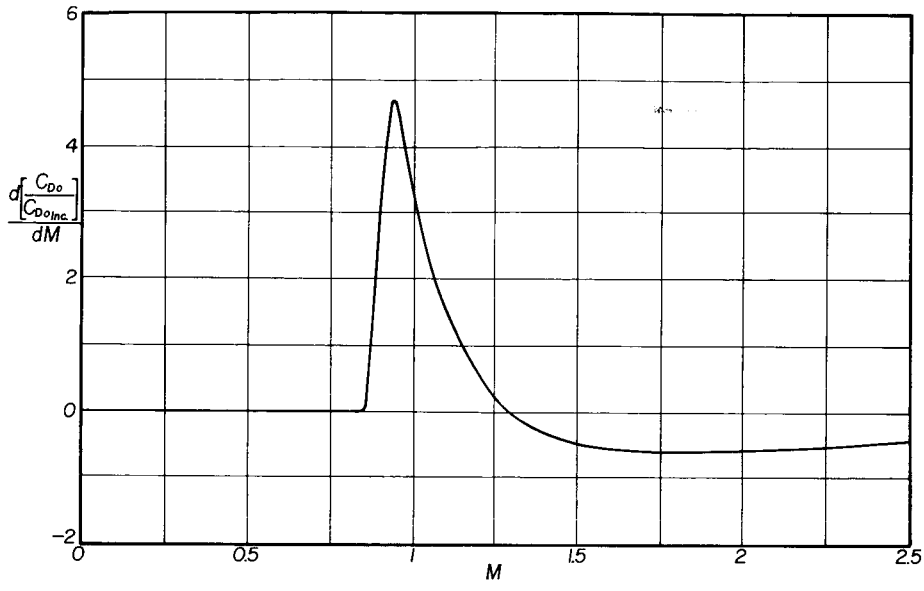

(a) Configuration A.

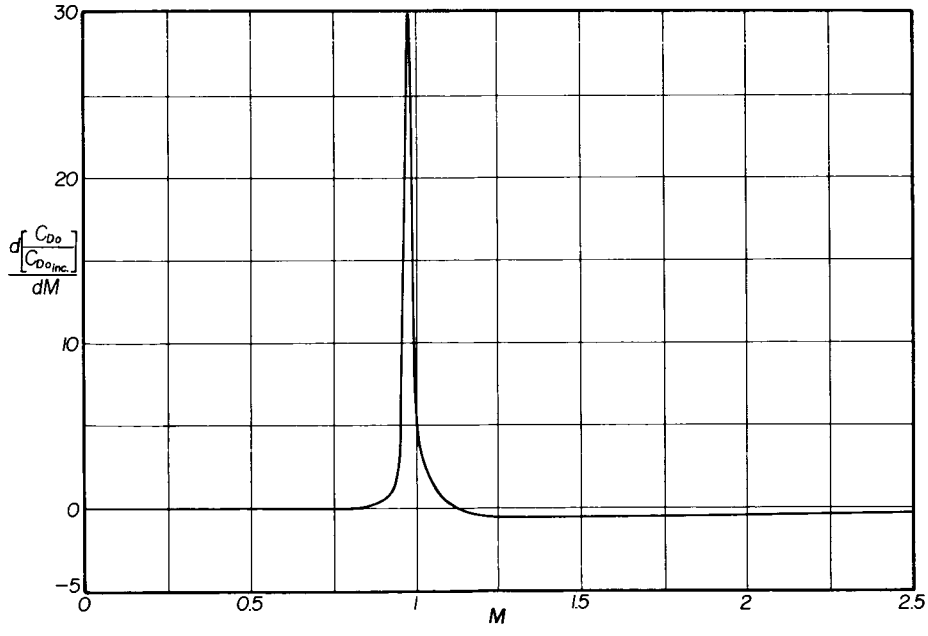

(b) Configuration B.

Figure 3.- Mach number derivative of the zero-lift drag coefficient as a function of the Mach number.

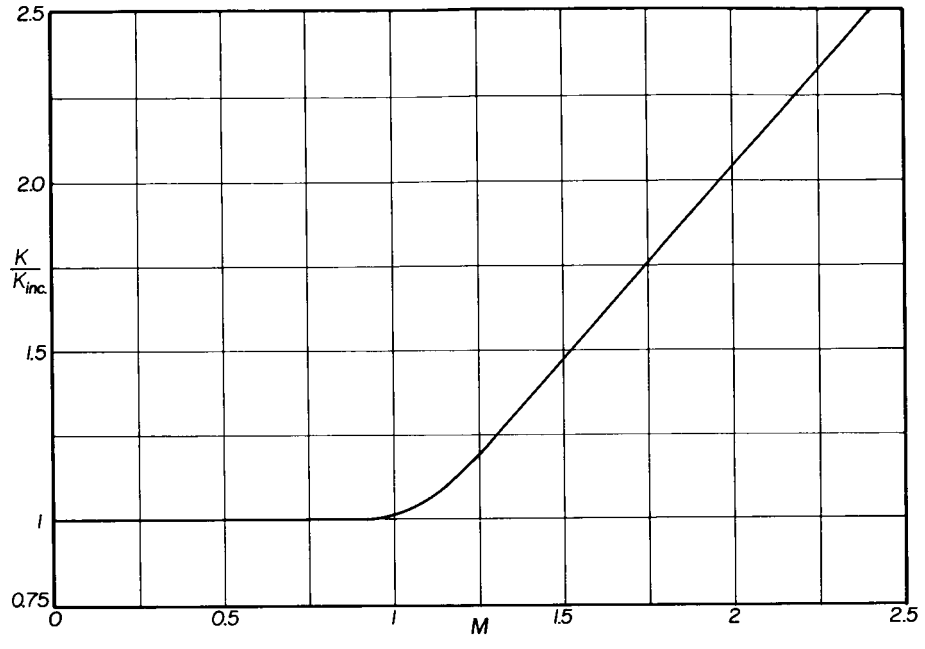

Figure 4.- Ratio of induced drag coefficient to square of lift coefficient as a function of Mach number (configurations A and B).

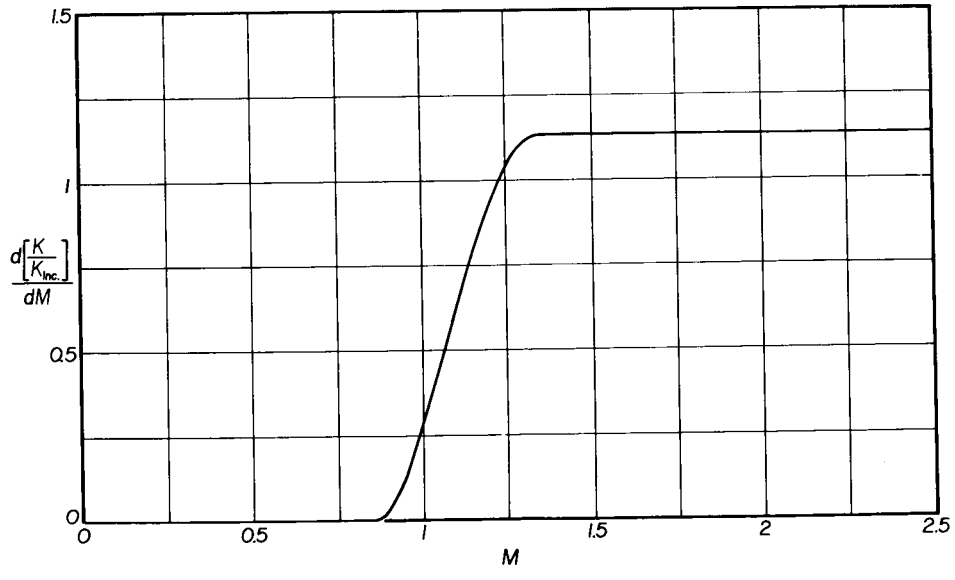

Figure 5.- Mach number derivative of ratio of induced drag coefficient to square of lift coefficient as a function of the Mach number (configurations A and B).

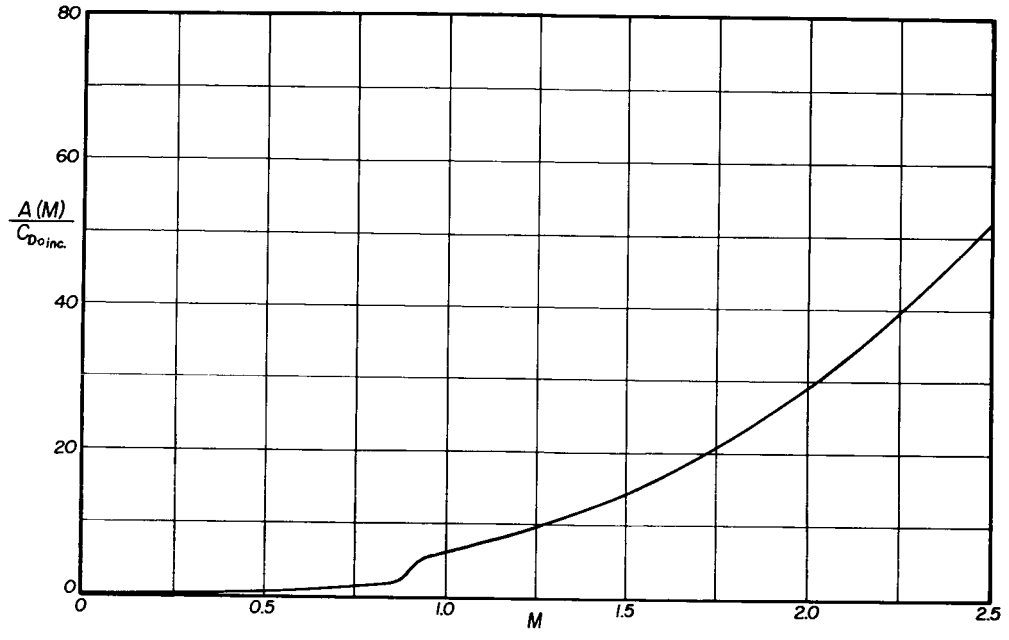

(a) Tropospheric flight.

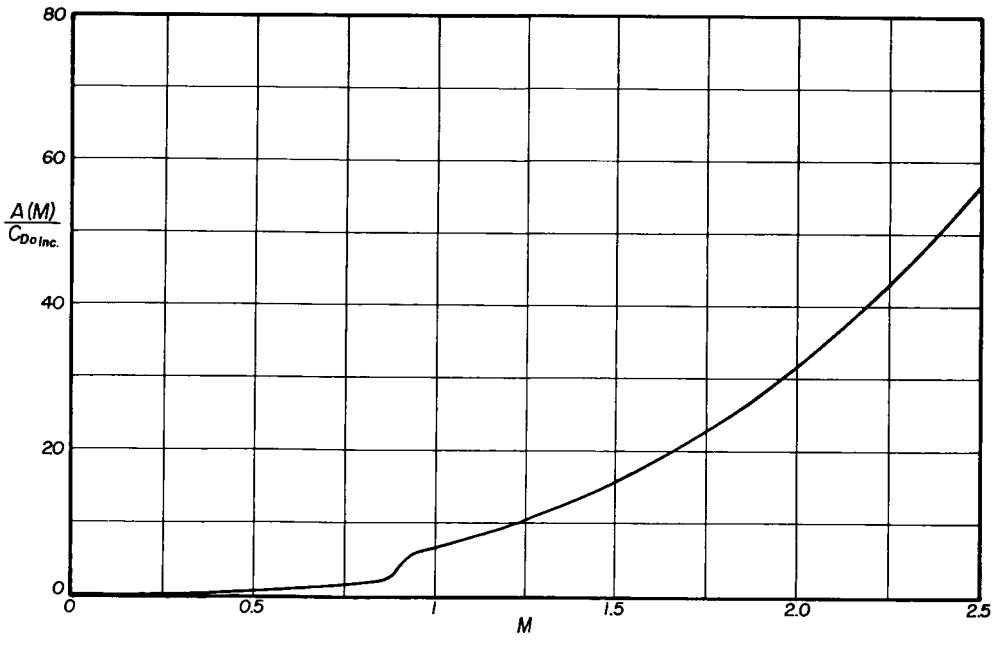

(b) Stratospheric flight.

Figure 6.- The function A(M) for configuration A.

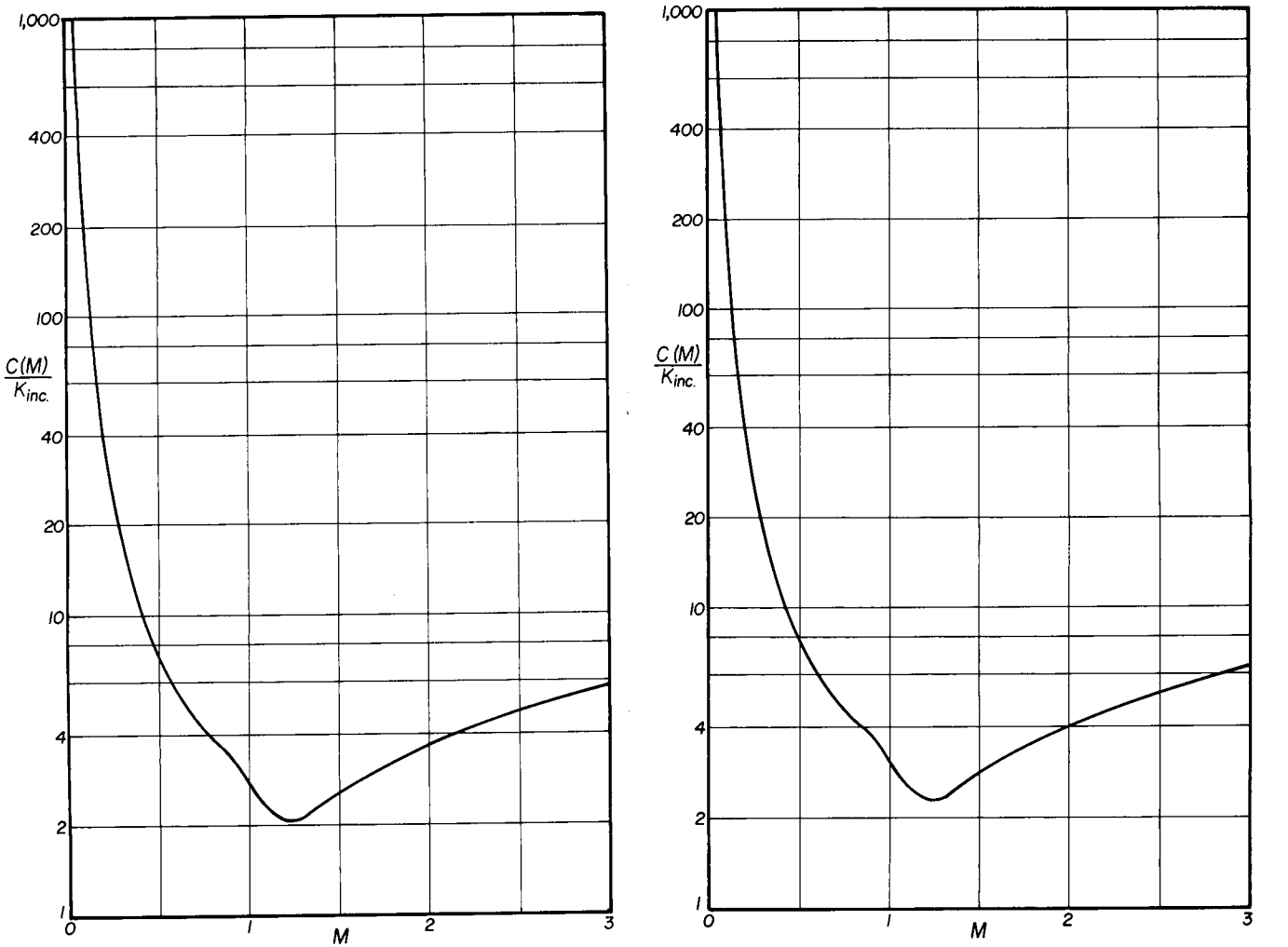

(a) Tropospheric flight.

(b) Stratospheric flight.

Figure 7.- The function C(M) for configurations A and B.

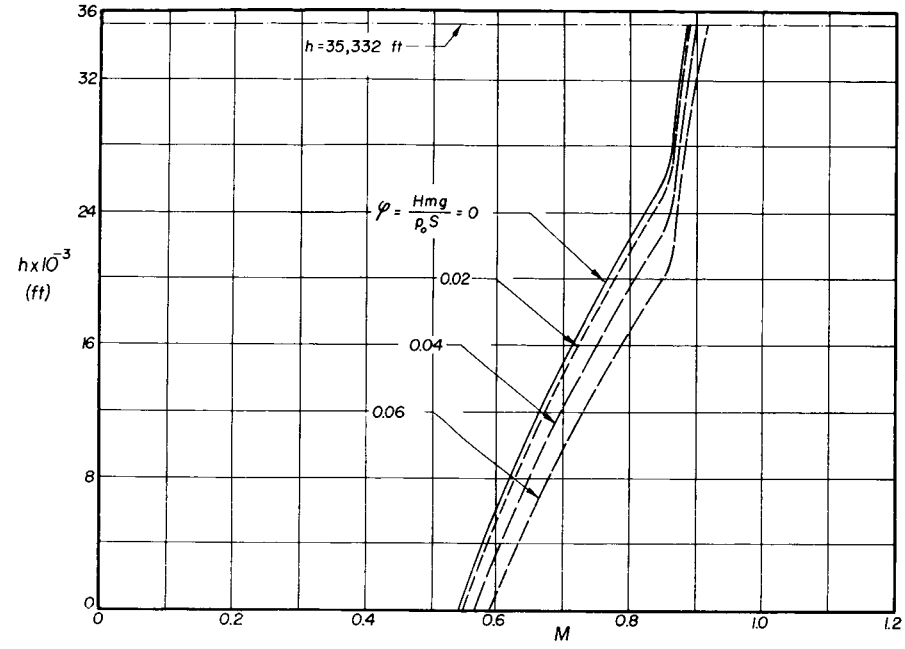

(a) Tropospheric flight.

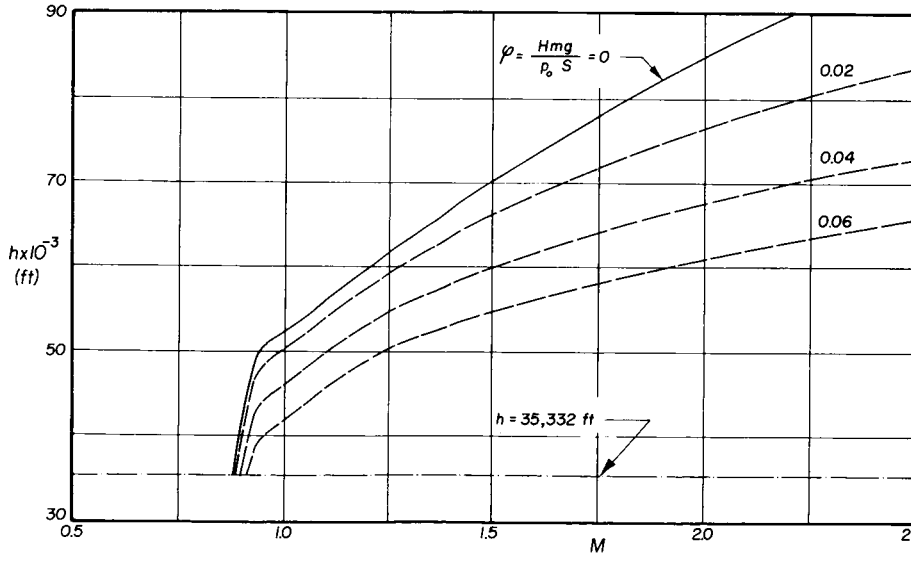

(b) Stratospheric flight.

Figure 8.- Relationship between altitude, Mach number, and parameter φ at points of the subarc flown with variable path inclination for configuration A.

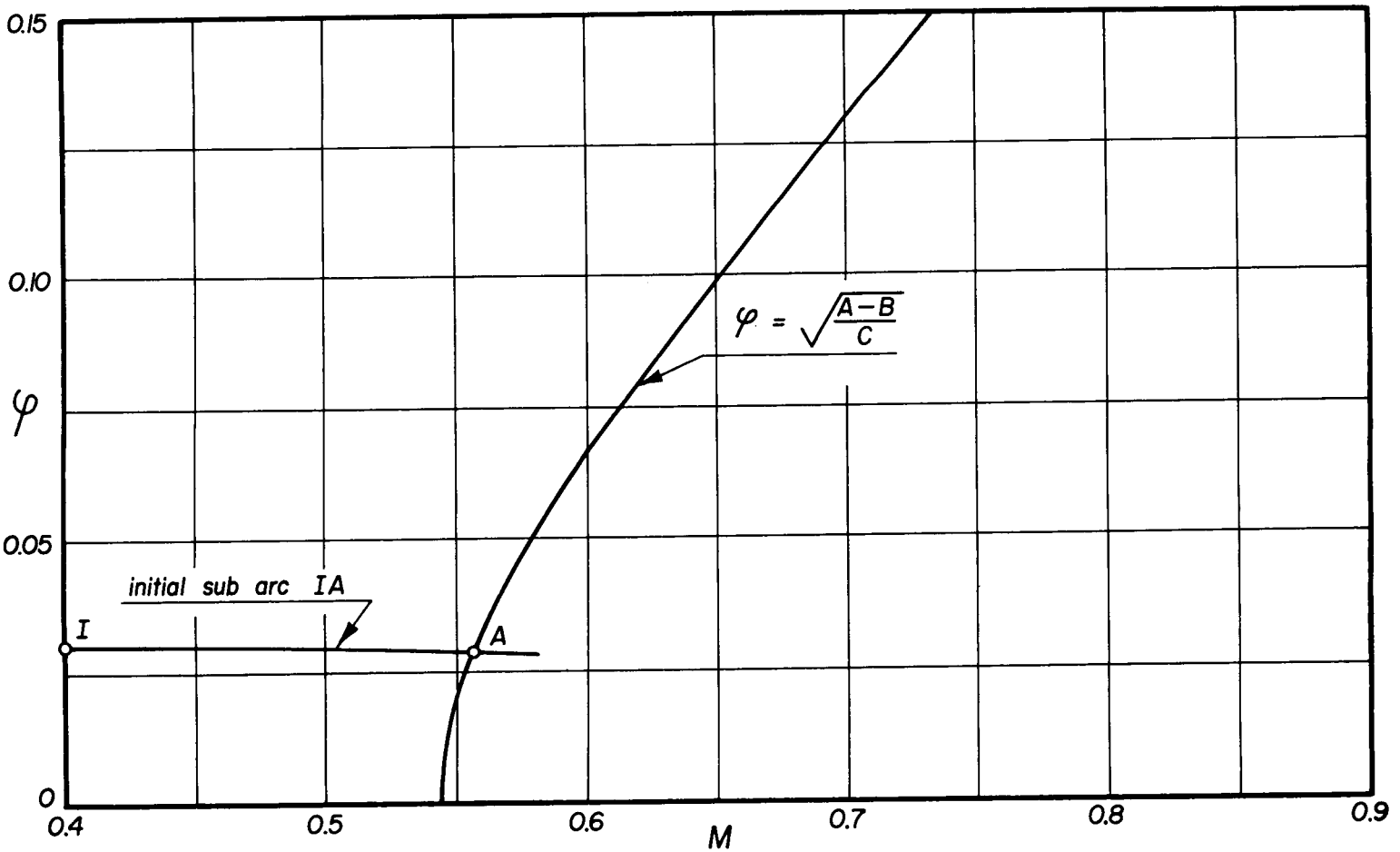

Figure 9.- Determination of coordinates of corner point A in the φ,M plane (configuration A; tropospheric flight).

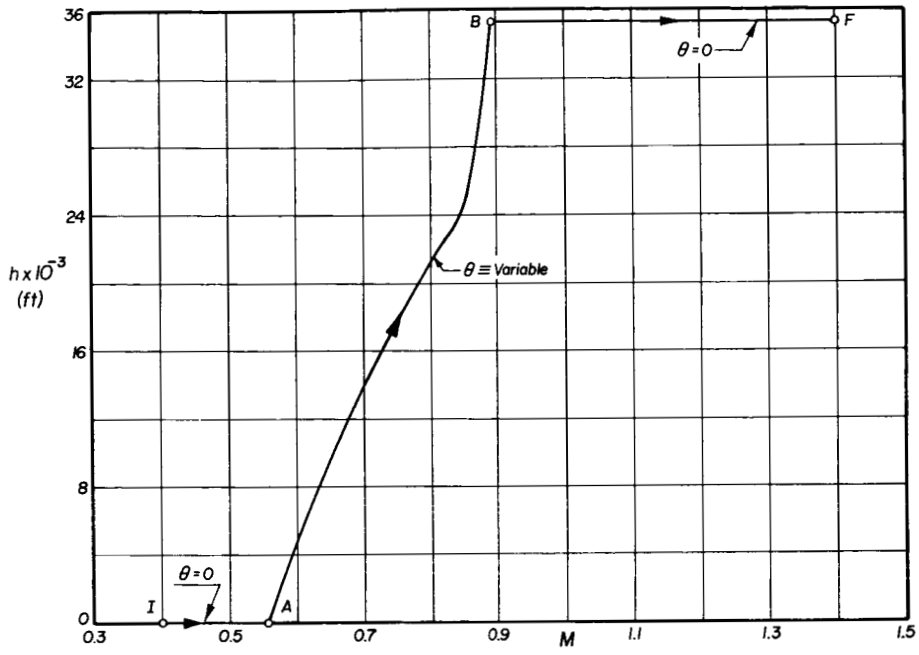

(a) Altitude-Mach number plane.

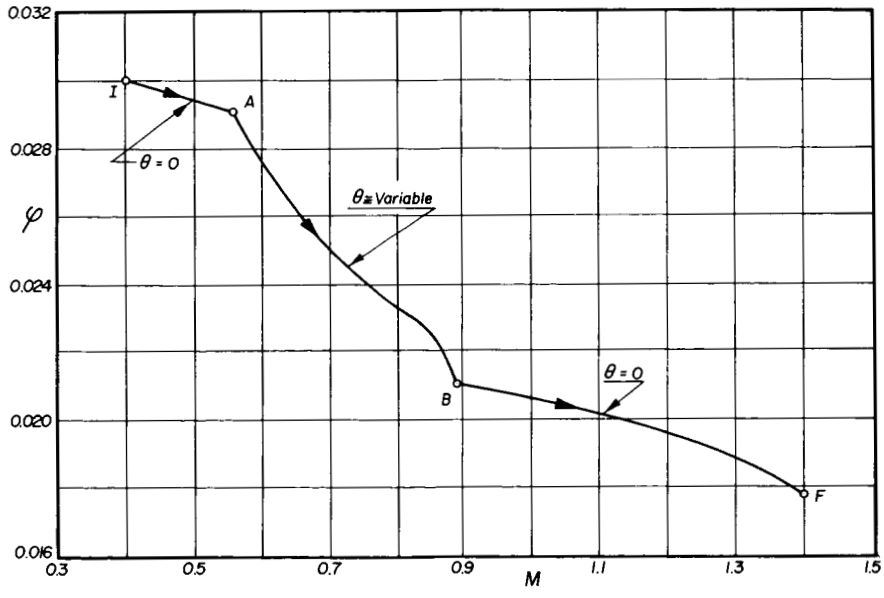

(b) Mass-Mach number plane.

Figure 10.- Particular extremal trajectory for configuration A in tropospheric flight.

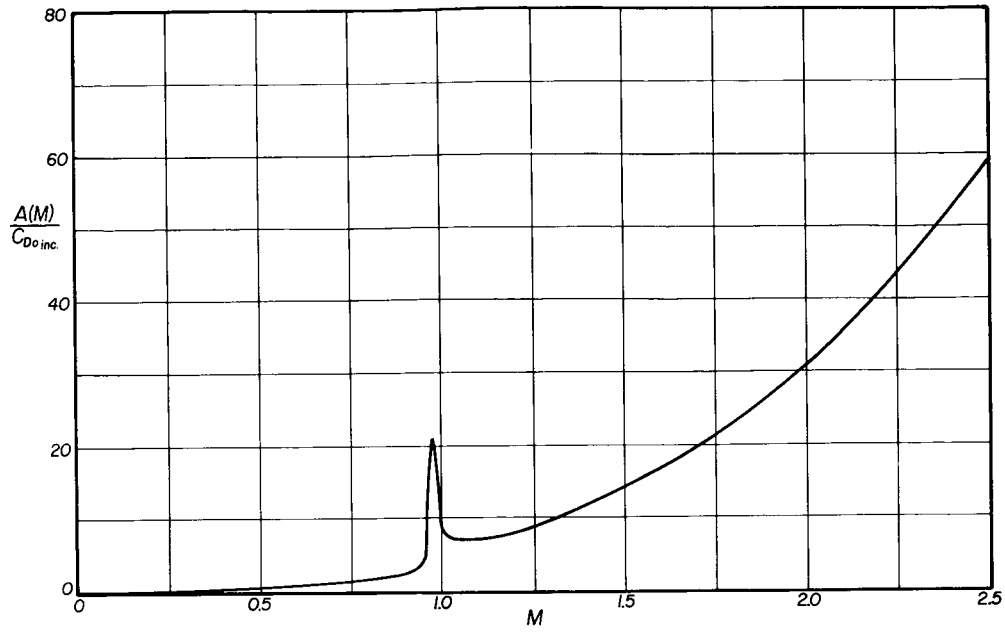

(a) Tropospheric flight.

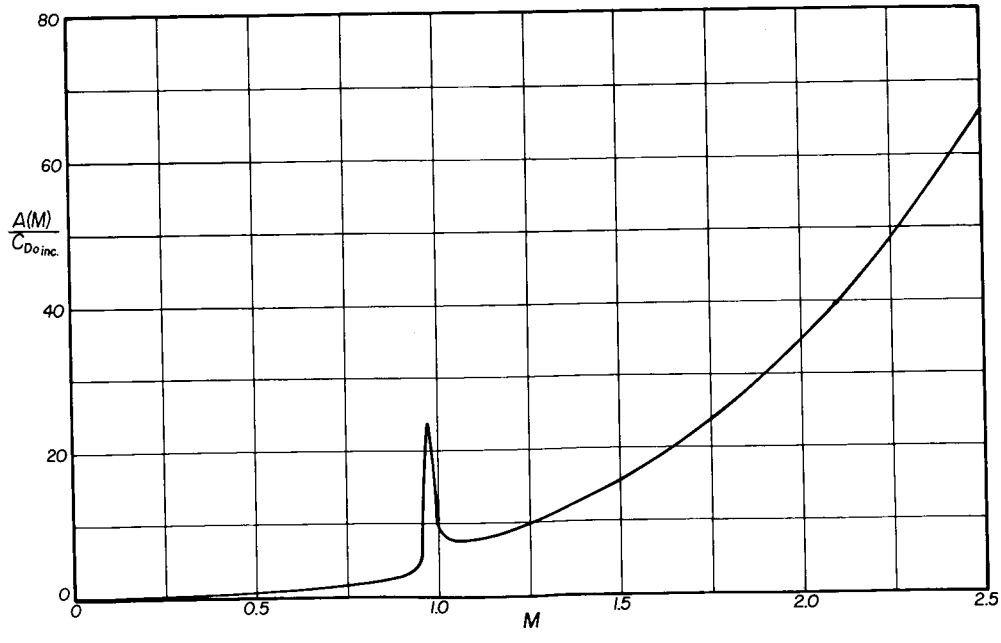

(b) Stratospheric flight.

Figure 11.- The function A(M) for configuration B.

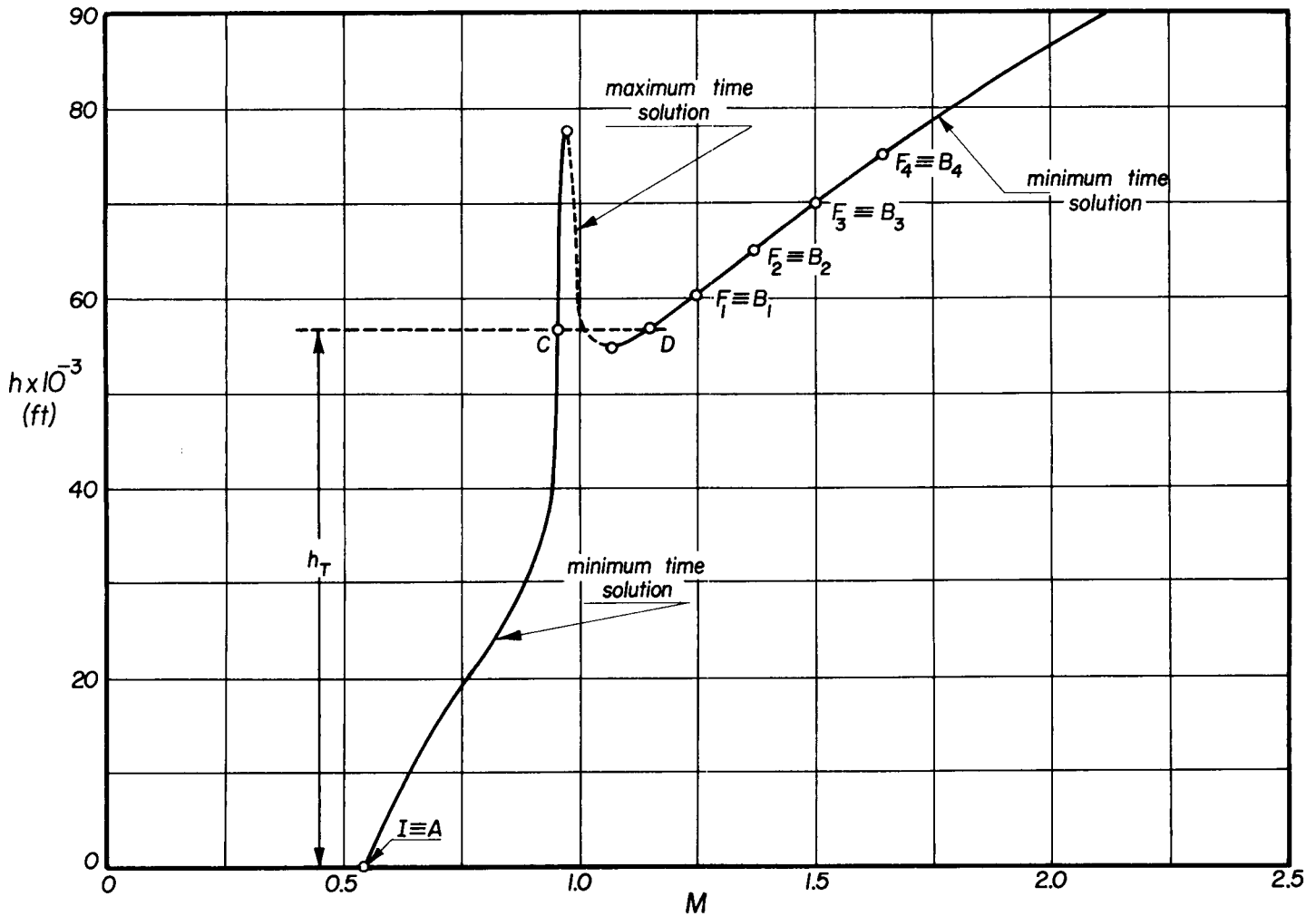

Figure 12.- Altitude-Mach number relationship at points of subarc flown with variable path inclination (configuration B; induced drag neglected).

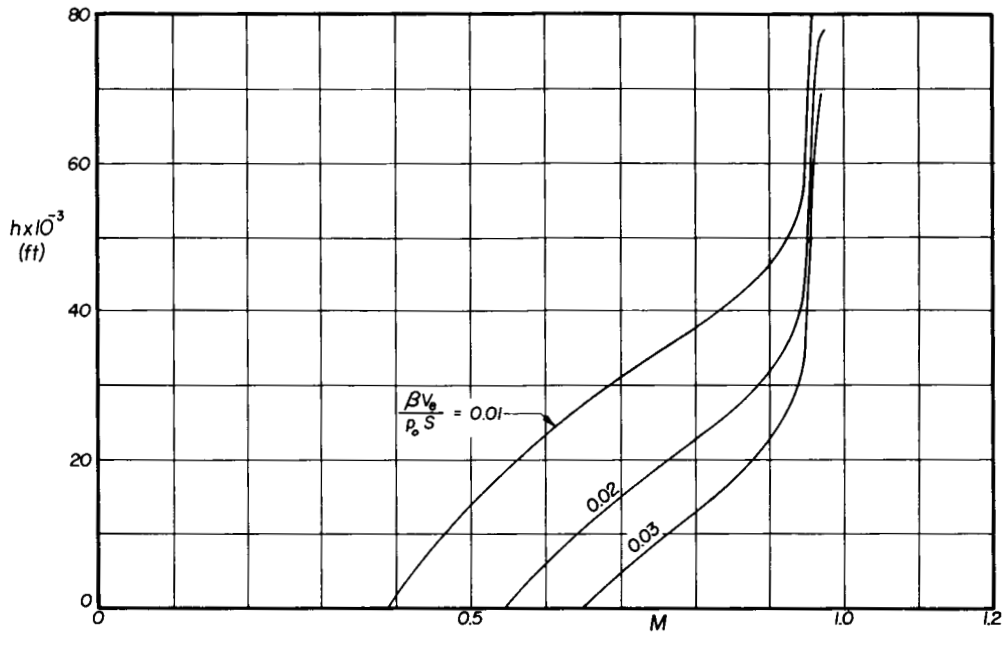

(a) Subsonic branch.

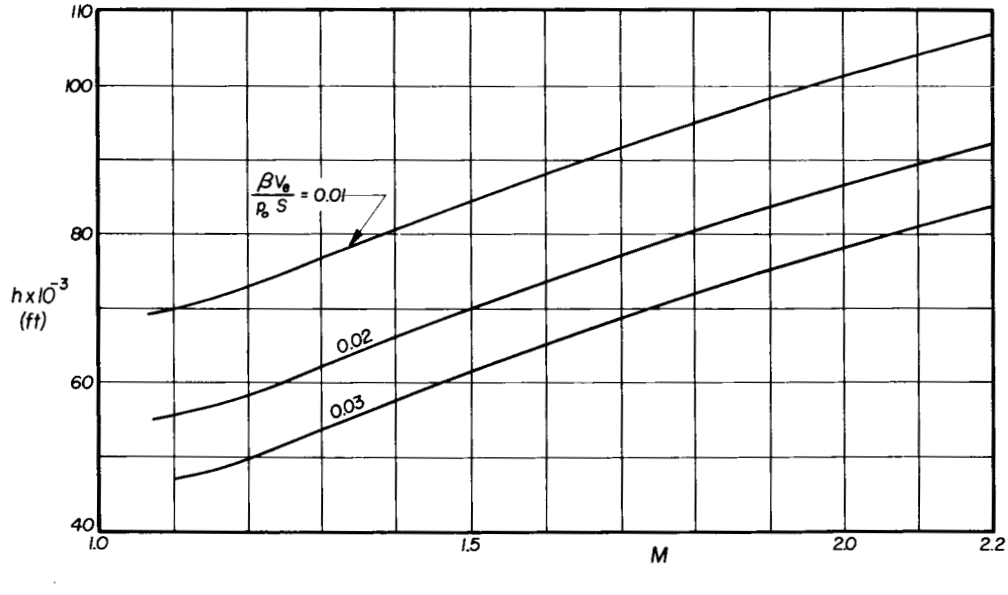

(b) Supersonic branch.

Figure 13.- Effect of thrust loading on Mach number-altitude relationship at points of two branches of the subarc flow with variable path inclination (configuration B; induced drag neglected).

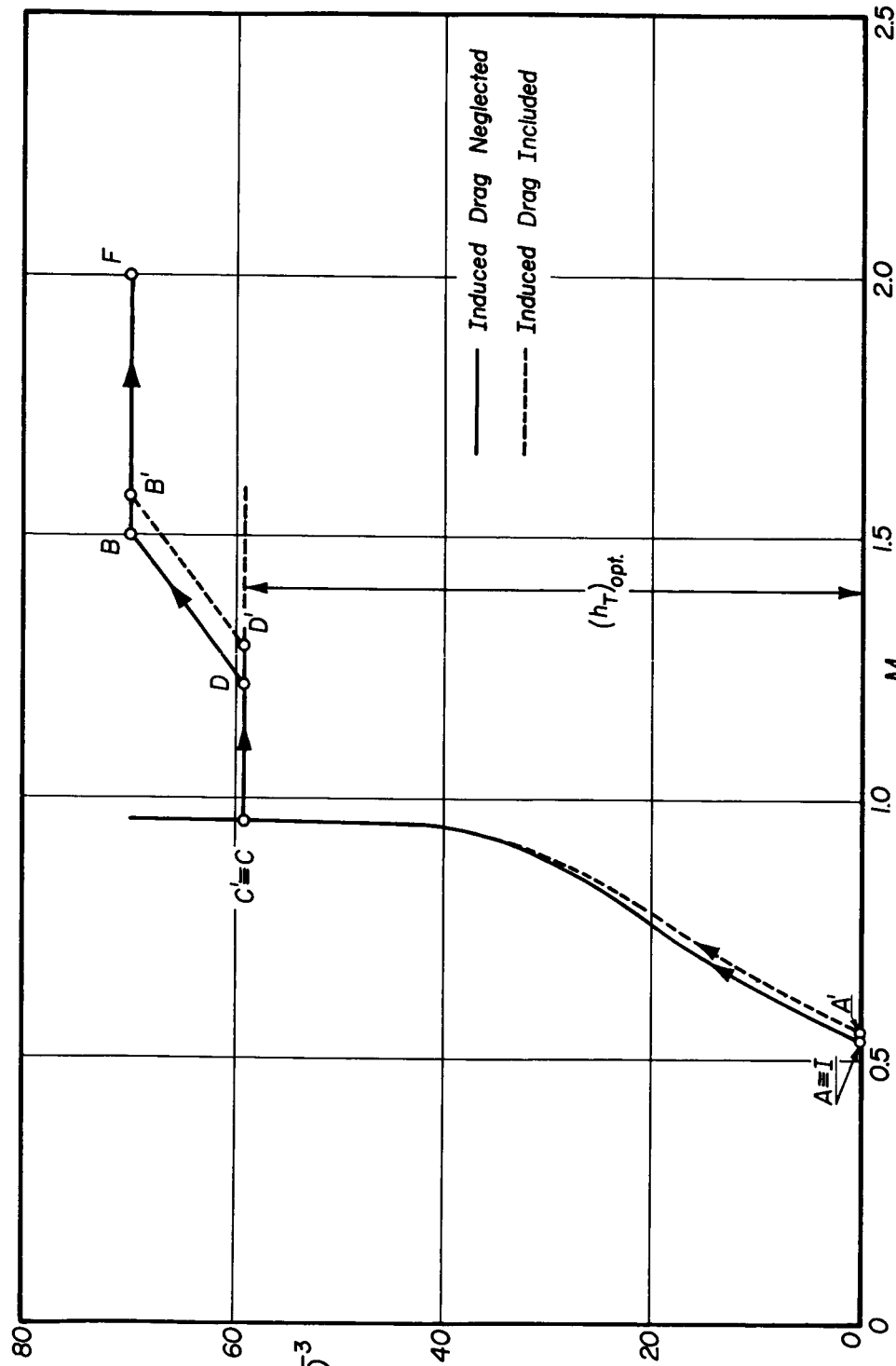

Figure 14.- Particular extremal trajectory in altitude-Mach number plane (configuration B).

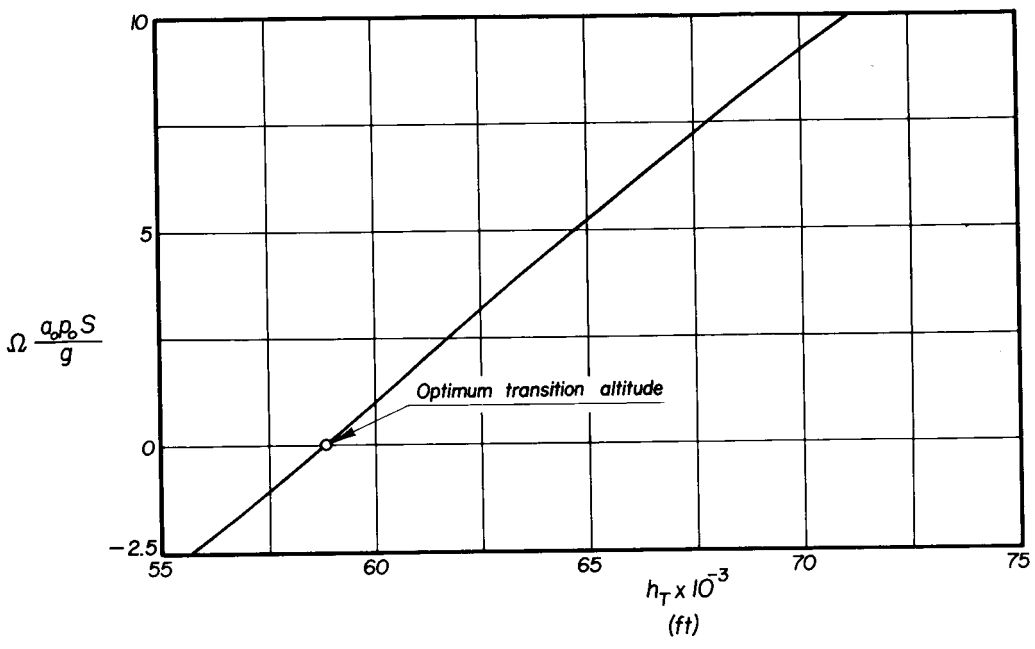

Figure 15.- Determination of optimum transition altitude (configuration B; induced drag neglected).

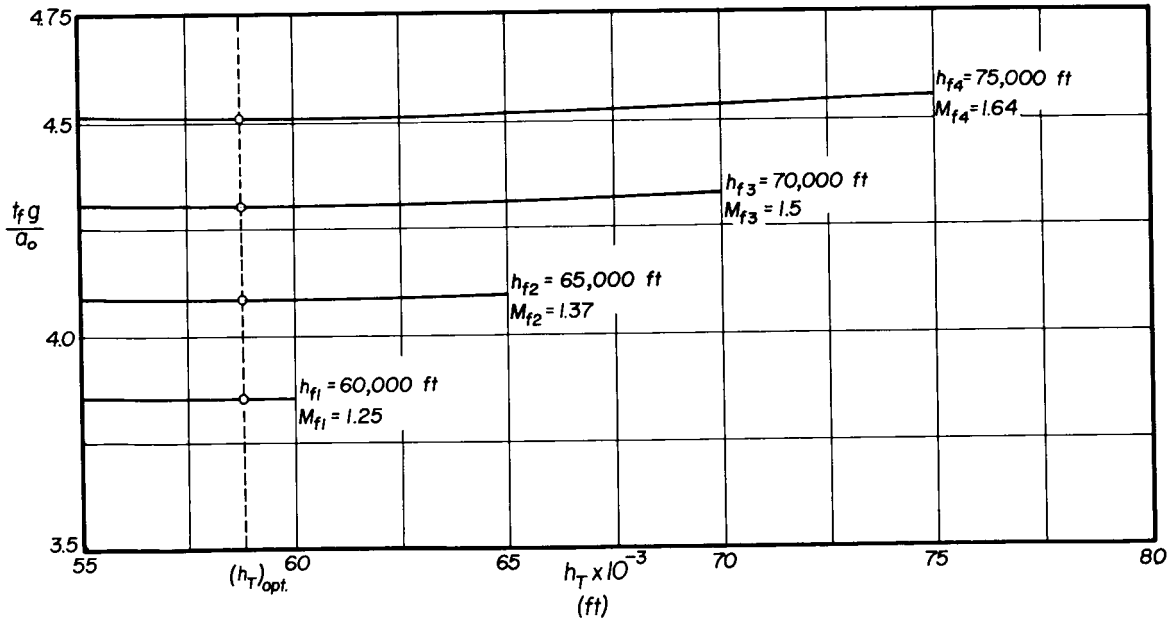

Figure 16.- Effect of transition altitude on time necessary to reach desired final point (configuration B; induced drag neglected).

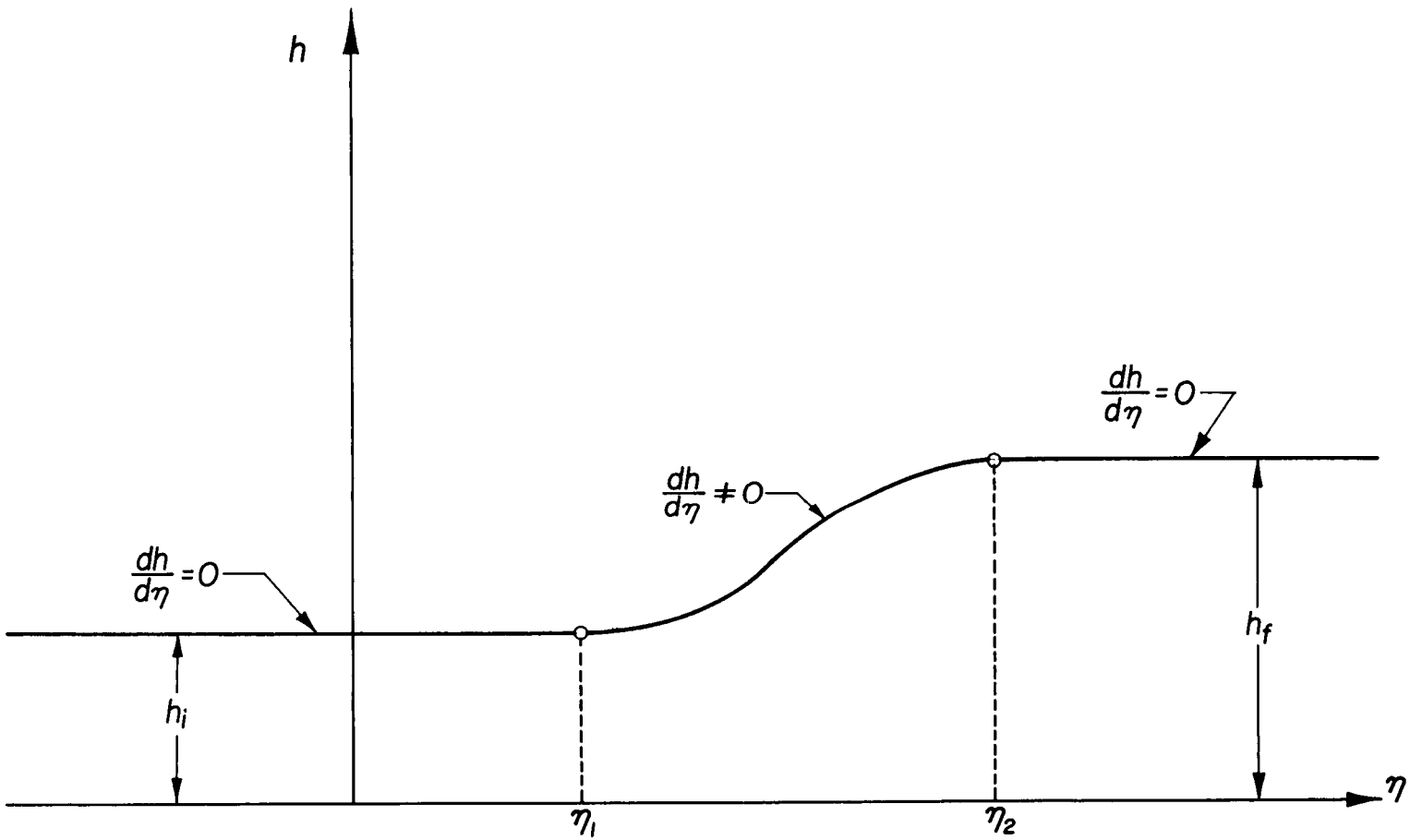

Figure 17.- Parametric representation of altitude for variational problem where $h_f \geqq h \geqq h_i$.

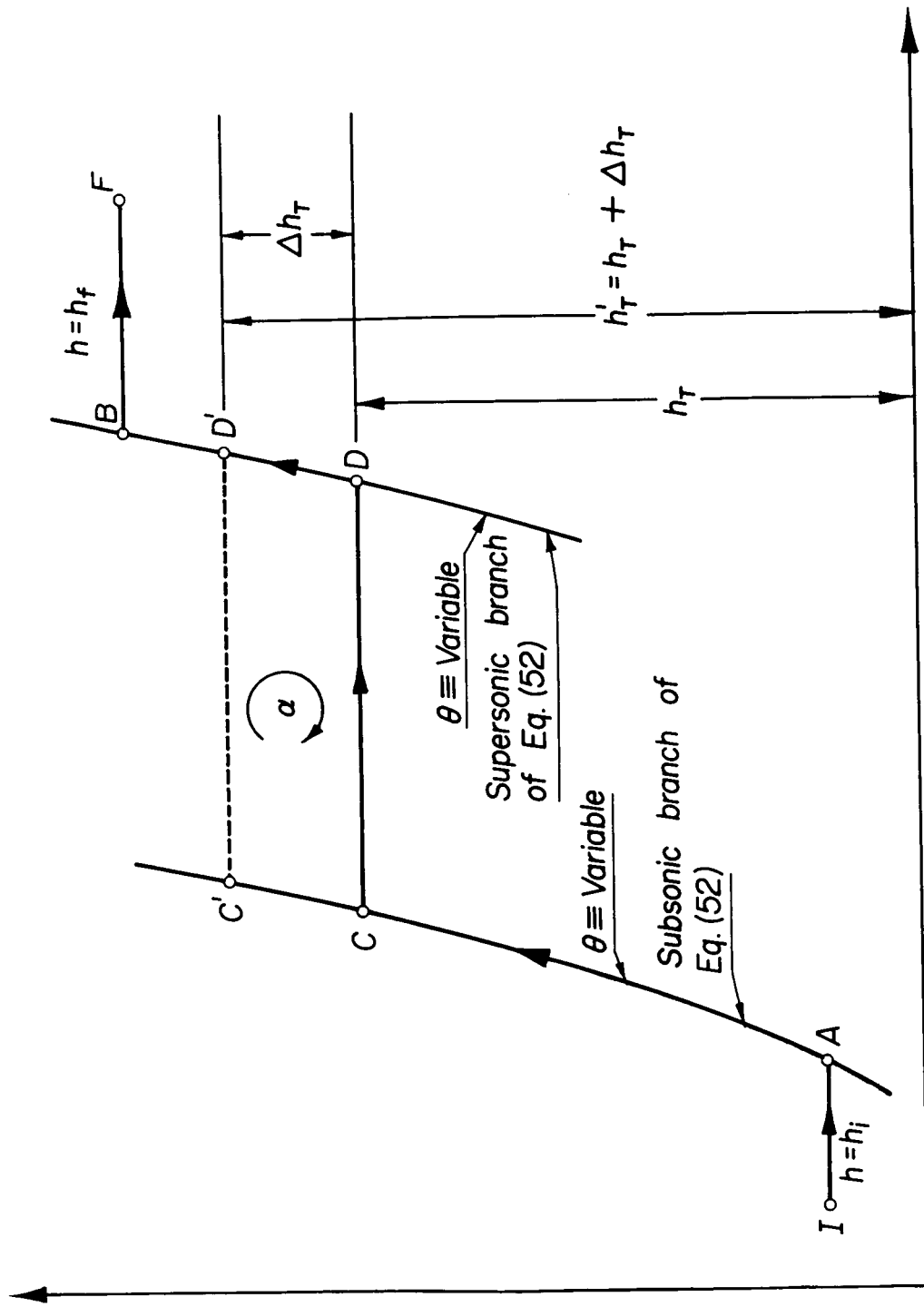

Figure 18.- Determination of optimum transition altitude (induced drag neglected).